



# HERCULES-2 Project

*Fuel Flexible, Near Zero Emissions, Adaptive Performance Marine Engine*

## Deliverable: **D7.2**

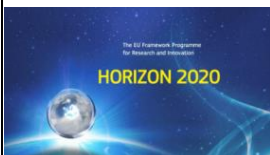
### Emission measurement systems for integrated after-treatment technologies

Revision final

Nature of the Deliverable: Report  
Due date of the Deliverable: 1.3.2018  
Actual Submission Date: 7.3.2018  
Dissemination Level: Public

Contributors: Timo Murtonen, Kati Lehtoranta, Päivi Aakko-Saksa, Olli Antson, Hannu Vesala, Päivi Koponen, Rasmus Pettinen  
VTT Technical Research Centre of Finland LTD

Work Package Leader Responsible: Jukka Leinonen (Wärtsilä Finland)



Start date of Project: 01/05/2015      Duration: 42 months

Grant Agreement No: **634135-HERCULES-2**

**HORIZON 2020**  
The EU Framework Programme for Research and Innovation



## TABLE OF CONTENTS

1	Executive Summary.....	3
2	Introduction.....	6
3	Desk-top studies.....	7
3.1	Development of regulation.....	7
3.2	Sulphur trioxide (SO <sub>3</sub> ) literature study.....	10
4	Measurement campaigns and methodology.....	13
4.1	Description of work.....	13
4.2	Particulate matter and particle number studies.....	16
4.2.1	PM measurement methods.....	16
4.2.2	PN measurement methods.....	21
4.2.3	Measurement campaigns.....	26
4.3	NH <sub>3</sub> measurement studies.....	29
4.3.1	NH <sub>3</sub> measurements methods.....	29
4.3.2	Measurements campaigns.....	31
4.4	Methane catalyst study.....	36
5	Results.....	38
5.1	PM and PN studies.....	38
5.1.1	Verification of movable PM-SDS at VTT's laboratory.....	38
5.1.2	Filter material comparison for PM measurements and role of back-up filters.....	39
5.1.3	Comparison of Pegasor PPS-M sensor and VTT's PN measurement system.....	41
5.1.4	PM and PN results from DF engine and in onboard ship campaigns.....	42
5.2	NH <sub>3</sub> sensor studies.....	44
5.2.1	NH <sub>3</sub> measurements at VTT's laboratory.....	44
5.2.2	NH <sub>3</sub> ship trial 1.....	47
5.2.3	NH <sub>3</sub> ship trial 2.....	49
5.2.4	NH <sub>3</sub> ship trial 3.....	52
5.3	Sulphur trioxide (SO <sub>3</sub> ) screening.....	55
5.4	Methane catalyst study.....	57
6	Conclusions.....	60
7	Acknowledgements.....	62
8	References.....	63

# 1 Executive Summary

In Workpackage 7 the subproject 7.4 with the title *Emission measurement systems for integrated after-treatment technologies* focuses to the challenges of sampling and measuring of exhaust gases and particles, the testing of potential gas sensors, and to a study of methane oxidation catalyst. The activities were directed to possible future needs caused by tightening emission limits, and measurements campaigns in ships. Cost-effective and reliable sensors for particle and gas measurements are needed for emission measurements and for the control of ammonia injection in NO<sub>x</sub> reduction units. Moreover, in natural gas engines some amounts of methane can end up in the exhaust gas. The methane catalyst study focused on decreasing this methane emission and on the regeneration experiments of the catalyst.

The research work in subproject 7.4 is a combination of experimental studies in laboratory and on cruising vessels. We have utilized VTT's catalyst test bench and measurement facilities for gas and diesel engines. These facilities are equipped with a versatile selection of gas and particle measurement systems such as Fourier transformation infrared (FTIR), laser diode spectroscopy (LDS), particle number counter (PNC) and micro gas chromatography (MicroGC) and sampling systems developed for SCR units.

Subproject 7.4 covered the following tasks:

- Desk-top work on emission regulation and sulphur trioxide (SO<sub>3</sub>) measurements methods
- Development of movable particulate matter (PM) sampling system for ships
- Filter material study
- PM and particle number (PN) measurements
- Ammonia (NH<sub>3</sub>) sensor measurements
- Screening of SO<sub>3</sub> experimentally
- The methane catalyst study

## SO<sub>3</sub> measurement methods and screening

The literature study on SO<sub>3</sub> describes direct and indirect SO<sub>3</sub> measurement methods, commercial products and test results. The challenges in measuring SO<sub>3</sub> are related to thermodynamical properties of SO<sub>3</sub> - H<sub>2</sub>SO<sub>4</sub> system in water containing flue gas matrix, to the representativity of sampling, and to tolerance of optical components to reactive gases. Below about 350 °C H<sub>2</sub>SO<sub>4</sub> is the dominant component and the proportion of SO<sub>3</sub> decreases with higher water contents and lower temperature. H<sub>2</sub>SO<sub>4</sub> condenses to cold surfaces and causes corrosion in process devices and SO<sub>3</sub> reaction products may accumulate on catalyst surfaces and gradually degrade catalyst's efficiency. The presence of SO<sub>3</sub> is also connected to the formation of visible plume (in the form of H<sub>2</sub>SO<sub>4</sub> aerosol) and increased particle emission.

The measurement methods for SO<sub>3</sub> can be divided to four categories:

- extractive direct analysis of SO<sub>3</sub>
- extractive indirect analysis of SO<sub>3</sub>
- extractive indirect continuous analysis of SO<sub>3</sub>
- cross-duct measurement and IR emission measurement by FTIR

Available commercial measurement systems cover the first three categories and they are all based on extractive sampling of exhaust gas. In a recent study several extractive indirect methods for SO<sub>3</sub>/H<sub>2</sub>SO<sub>4</sub> analysis were compared in laboratory and in process conditions. Result of the study was that if extracted gaseous SO<sub>3</sub>/H<sub>2</sub>SO<sub>4</sub> is fed through a teflon tube packed with NaCl or KCl salts, the method gave reliable results without any significant interference with SO<sub>2</sub>.

In laboratory conditions very low limit of detection (LOD) can be obtained for direct SO<sub>3</sub> measurements. Indirect methods can be utilized if continuous monitoring of SO<sub>3</sub> contents is not required. In a recent study a cross-duct measurement of SO<sub>3</sub> based on FTIR method indicated that the method can in principle be used for direct in-situ SO<sub>3</sub> analysis. However, testing in realistic conditions with 4 m and 14 m cross-duct lengths could not give definitive answer on the capability of the method.

SO<sub>3</sub> screening was carried out for supporting the SO<sub>3</sub> literature study. From the on-board results, exhaust SO<sub>3</sub> concentrations were calculated based on the analysed sulphates from filters. Conditions in our extractive filter sampling favored condensation of sulphuric acid, and also other non-volatile sulphates are collected. For two marine engines running on HFO, the results indicated that below 1% of SO<sub>2</sub> converted to SO<sub>3</sub>, while almost 4% for one engine.

### **PM and PN studies**

PM emissions were measured according to ISO 8178-1:2006 standard. In 2017 a new version of the standard was introduced (ISO 8178-1:2017). New version includes more strict specifications for PM measurement and includes requirements for PN measurement. The PN measurements of this project are performed according to the latest standard.

PM measurement of large engines is based on a partial-flow dilution of the exhaust gas. Standard describes several possible technical solutions for these dilution systems. VTT uses AVL 472 Smart Sampler for partial-flow PM sampling instrument consist of two units, the filter holder unit and flow control unit, which also includes all the needed electronics. AVL instrument is very large and heavy (control unit 73 x 64 x 164 cm, 245 kg and dilution unit 75 x 56 x 153 cm, 60kg) and therefore not very suitable for all field measurements. At VTT, a small movable Ship Dilution System (PM-SDS) was designed and built-up in the Hercules-2 project. PM-SDS uses the same measurement principle as AVL Smart Sampler. The size for the sampling unit is 60 x 40 x 25 cm and for the control unit 86

x 60 x 43 cm. Weights for the units are ca. 20 kg (sampling unit), 30 kg (control unit) and 10 kg (pump).

Different filter materials were studied in on-board measurements and with dual-fuel (DF) marine engine. PM sampling is typical in Europe using Teflon (PTFE) bonded glass fiber filters, while US EPA requires use of PTFE filters. We studied four types of filter materials, two PTFE-types, one PTFE bonded glass fiber and one quartz quality filters. As a conclusion, PTFE bonded glass fiber filters, and particularly quartz filters, tend to collect more material than the PTFE filters. However, at low PM concentrations this difference was not always consistent.

PM and PN measurements were performed on two on-board measurements campaigns. Three engines were measured using heavy fuel oil (HFO) and one of the engines with marine gas oil (MGO). In addition to on-board campaigns, a dual-fuel marine engine was measured using natural gas and LFO. Results point out that fuel quality has significant influence on PM and PN emissions. Switching from HFO to low sulphur MGO or LFO decreases the PM emission roughly by 50% and further on using natural gas reduces PM emissions by over 85% compared to LFO. On ships the PM reduction over the scrubber was 17-45%. The PN emissions (solid particles) before and after the scrubber were on the same level. With MGO, the PN emission were decreased by ca. 90% in comparison with HFO. With dual fuel engine the PN emissions with natural gas were 99% lower compared to LFO.

PN measurements also included comparison of legislative PN measurement method and Pegasor PPM-S particle sensor. Measurements were performed with DF engine in diesel and DF-modes using multiple engine loads. Results revealed that particle sensor needs application specific calibration for accurate results.

### **NH<sub>3</sub> studies**

Comparison of different NH<sub>3</sub> measurement techniques were performed at VTT's lab and in on-board measurements. The performance on NH<sub>3</sub> sensors was the main interest. Since LDS and FTIR methods are accepted for NH<sub>3</sub> measurement according to ISO 8178-1:2017, the Dephi NH<sub>3</sub> sensor was compared with those methods. The sensor is designed for automotive applications using clean fuels and comparison measurements with diesel bus showed that the results with LDS and sensor are equal. With FTIR the measured concentrations were slightly lower. With natural gas applications the sensor gives significantly lower concentrations compared to LDS and FTIR though the sensor response is linear in comparison with other instruments. It needs to be highlighted that the sensor is not designed for natural gas applications.

Three on-board measurements campaigns were performed with the sensor. One of those was comparison measurement with FTIR and two others a long-term test on ships using HFO and low

sulphur ( $S < 0.1\%$ ) residual fuel. Comparison measurements with FTIR were carried out with HFO and MGO. Results showed that extractive FTIR method is very sensitive to sulphur dioxide ( $SO_2$ ) when measuring  $NH_3$ . If  $SO_2$  is present in the exhaust gas, ammonium sulphate forms in the sampling system and the  $NH_3$  values measured by FTIR are underestimated. The long-term campaigns showed that  $NH_3$  sensor has potential to be used for monitoring  $NH_3$  in harsh conditions if precautions are used for protecting the sensor.

### **Methane catalyst study**

Oxidation catalyst is one way to reduce the methane emission but the  $SO_2$  and water present in the exhaust gas has found to inhibit the oxidation of methane and therefore a regeneration procedure needs to be developed in order to maintain the catalyst efficiency. In this work the regeneration of a methane oxidation catalyst (MOC) by  $H_2$  was studied.

Study was performed with passenger car natural gas engine using a special test facility designed for catalyst studies. The target was to mimic the emission levels of a relevant power plant engine and the engine was operated with lean air-to-fuel mixture. Experiments were performed with a methane oxidation catalyst ( $Pd/Pt-Al_2O_3$ ) at exhaust temperature of  $500^\circ C$  with an additional experiment at  $550^\circ C$ . The experiments included ageing the catalyst for 190 hours and regenerations every 20 hours. Regeneration was performed by feeding  $H_2$  into the exhaust gas. During the ageing, a small amount of  $SO_2$  was fed in to the catalyst.

This study showed that the  $H_2$  assisted regeneration could be one way to recover the methane oxidation catalyst's performance. However, before taking this method to real applications, there are several issues to be studied further.

## **2 Introduction**

One of the main objectives of Hercules-2 project is: *Achieving near-zero emissions, via combined integrated aftertreatment of exhaust gases*. The workpackage group IV: *Near-Zero Emissions Engine* focuses on this objective through two workpackages: *WP7 On-engine aftertreatment systems*, and *WP8 Integrated SCR and Combined SCR & Filter*.

In WP7 the subproject 7.4 with the title *Emission measurement systems for integrated after-treatment technologies* focuses to the challenges of sampling and measuring of exhaust gases and particles, the testing of potential gas sensors, and to the testing of methane catalyst materials in test rigs with engines. The activities were directed to possible future needs caused by tightening emission limits and measurements campaigns in ships. Cost-effective and reliable sensors for

particle and gas measurements are needed for emission monitoring and for the control of urea dosing in NO<sub>x</sub> reduction units. Moreover, in natural gas engines some amounts of methane can end up in the exhaust gas. One way to decrease the methane emissions is the utilization of an oxidation catalyst. However, SO<sub>2</sub> and water present in the exhaust gas has been found to inhibit the oxidation of methane. The methane catalyst study focused to the development of a regeneration procedure for these catalyst materials.

Subproject 7.4 covered the following tasks:

- Desk-top work on emission regulation and SO<sub>3</sub> measurements methods
- Development of small size movable PM sampling system for ships
- Filter material study for PM measurements
- PM and PN measurements from exhaust of two ships (on-board) and a DF engine
- NH<sub>3</sub> sensor measurements
- Screening of SO<sub>3</sub> experimentally
- The methane catalyst study

The research work in subproject 7.4 is a combination of experimental studies in laboratory and in cruising vessels. We have utilized VTT's catalyst test bench and measurement facilities for gas and diesel engines. These facilities are equipped with a versatile selection of gas and particle measurement systems such as FTIR, LDS and MicroGC and sampling systems developed for SCR units. The facilities include also standard gravimetric particle measurement systems, and instruments such as electrical low pressure impactor (ELPI) and condensation particle counter (CPC) for particle size distribution and number determination with predefined cut-off limit.

In addition to experimental work, overview of emission regulations and , a literature review on SO<sub>3</sub> was conducted. During the planning phase of the workpackage 7.4 VTT considered to include an experimental study on the development of a real-time and direct SO<sub>3</sub> measurement system. The system was dedicated to SO<sub>3</sub> studies in selective catalytic reduction (SCR) units and in exhaust channel of marine diesel engines but could be utilized also in power plant boilers. This was considered to be important as real time data offers many advantages in comparison to offline and indirect analysis methods. However, in the early phase of the Hercules-2 project, it was decided to put the development of SO<sub>3</sub> measurement facility aside in the workpackage 7.4. Experimental study on SO<sub>3</sub> in this workpackage is related to the estimation of SO<sub>3</sub> amount needed to accumulate the observed sulfate (SO<sub>4</sub>) in PM as described in chapter 5.3

## **3 Desk-top studies**

### ***3.1 Development of regulation***

IMO, the International Maritime Organisation, is a specialised United Nations agency which is responsible for regulating international shipping, preventing marine pollution, and handling maritime security issues (EPRS 2016). The current rules of the prevention of ship pollution is contained in the

“International Convention on the Prevention of Pollution from Ships” known as MARPOL 73/78 created by International Maritime Organization (IMO).

In 1997 the Marpol Convention has been amended by the 1997 Protocol which includes Annex VI titled “Regulations for the Prevention of Air Pollution from Ships”. MARPOL Annex VI (IMO/Marpol 2018) sets limits on nitrogen oxide (NO<sub>x</sub>), and sulphur oxides (SO<sub>x</sub>) emissions from ship exhausts, and prohibits deliberate emissions of ozone depleting substances.

In the MARPOL Annex VI the rules for controlling NO<sub>x</sub> emissions from ships are collected in the document NO<sub>x</sub>-Regulation 13 (IMO 2017) and in the NO<sub>x</sub> Technical Code 2008 (IMO 2018). These rules have been amended by the Marine Environment Protection Committee (MEPC) of IMO by resolution MEPC.177(58) and by resolution MEPC.251.(66). Regulation of SO<sub>x</sub> and PM are specified in Regulation 13 and 14 in the MARPOL Annex VI. Ship owner can prove the compliance of the engine to these rules by acquiring an Engine International Air Pollution Prevention (EIAPP) Certificate which is prepared by the engine manufacturer or a classification society.

In addition to the mentioned emission limits, MARPOL Annex VI defines specific control areas where more stringent emission levels are required for NO<sub>x</sub> and SO<sub>x</sub>. However, there is no regulation for particulate matter from ships operating in these specific emission control areas or other sea areas. Emission control areas are situated around US and Canada coastline, The North Sea and the Baltic Sea coastline (IMO 2018). This regulation has been introduced according to the following schedule:

- Baltic Sea (SO<sub>x</sub>: adopted 1997 / entered into force 2005; NO<sub>x</sub>: 2016/2021)
- North Sea (SO<sub>x</sub>: 2005/2006; NO<sub>x</sub>: 2016/2021)
- North American ECA, including most of US and Canadian coast (NO<sub>x</sub> & SO<sub>x</sub>: 2010/2012).
- US Caribbean ECA, including Puerto Rico and the US Virgin Islands (NO<sub>x</sub> & SO<sub>x</sub>: 2011/2014).

The NO<sub>x</sub> emission and fuel sulphur limit values designated as presented in MARPOL Annex VI are shown Figure 1 and Figure 2 (DieselNet 2018). The emission limit values defined by Tier III apply to the specific emission control areas.



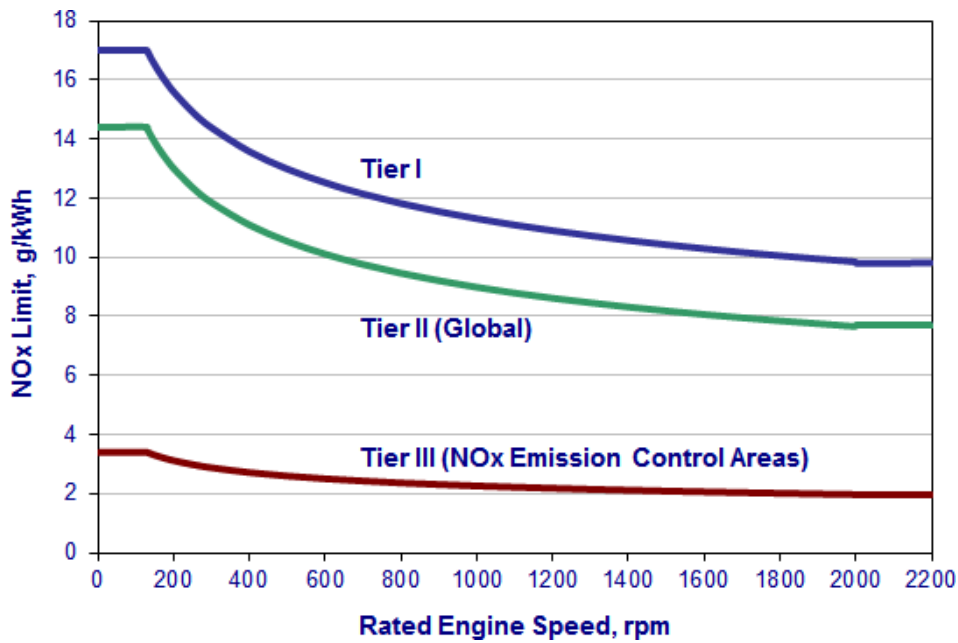


Figure 1. NO<sub>x</sub> emission limit values for global and specific emission control areas (DieselNet 2018).

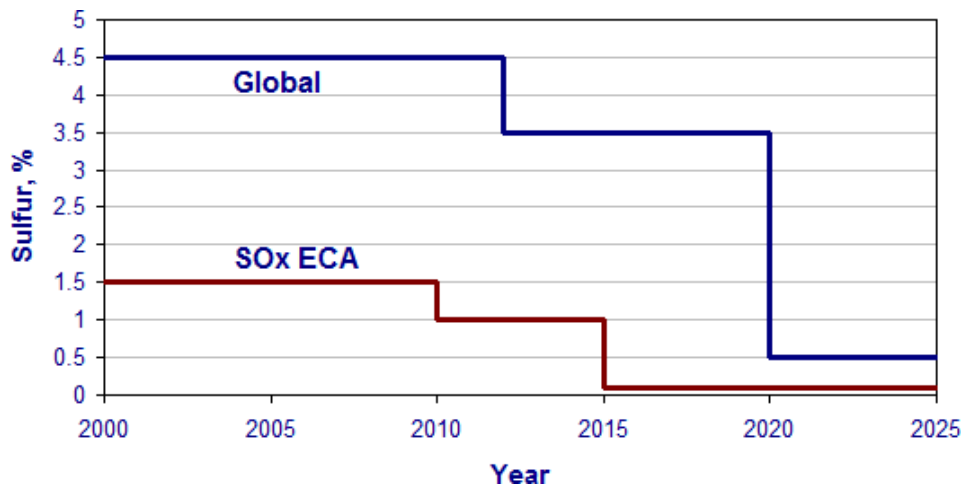


Figure 2. Fuel sulphur limit values for global and specific emission control areas (DieselNet 2018).

In European Union the current regulation concerning gaseous and particulate pollutant emission limits and type-approval for internal combustion engines for non-road mobile machinery has been prepared by European Parliament and Council in 2016 (EUR-Lex 2016). This regulation contains emission limit values for gases (CO, HC, NO<sub>x</sub>), and for particle mass and particle number emissions also for inland waterway vessels. Concerning the field campaigns in the Workpackage 7.4 we have carried out particle matter and number measurements based on this regulation and on the ISO8178 standard.

### **3.2 Sulphur trioxide (SO<sub>3</sub>) literature study**

This literature study describes direct and indirect SO<sub>3</sub> measurement methods, some commercial products and test results. In this literature study the following analysis methods are considered:

- extractive direct analysis of SO<sub>3</sub>
- extractive indirect analysis of SO<sub>3</sub>
- extractive indirect continuous analysis of SO<sub>3</sub>
- cross-duct measurement and IR emission measurement by FTIR
- some commercial systems for SO<sub>3</sub> analysis

The background of the planned study is the well-known formation of SO<sub>3</sub> in the burning process in boiler or in cylinder as an oxidation result of SO<sub>2</sub>. Typical concentration of SO<sub>3</sub> is 1-2 % of SO<sub>2</sub> concentration or about 1-25 ppm in boilers (EPRI 2004). SO<sub>3</sub> can be formed from SO<sub>2</sub> also in SCR unit on catalyst surfaces. In wet exhaust gas atmosphere SO<sub>3</sub> converts rapidly to H<sub>2</sub>SO<sub>4</sub> depending on temperature and water contents. H<sub>2</sub>SO<sub>4</sub> condenses to cold surfaces and causes corrosion in process devices. In SCR unit SO<sub>3</sub> can also react with extra NH<sub>3</sub> and form harmful ammonium sulphate (NH<sub>4</sub>)<sub>2</sub>SO<sub>4</sub> or ammonium bisulphate (NH<sub>4</sub>HSO<sub>4</sub>) (Srivastava 2005). These reaction products may accumulate on catalyst surfaces and gradually degrade catalyst's efficiency. The presence of SO<sub>3</sub> is also connected to the formation of visible plume (in the form of H<sub>2</sub>SO<sub>4</sub> aerosol) and increased particle emission (EPRI 2004).

At VTT direct SO<sub>3</sub> measurement technology has been studied earlier in national MMEA research program (Measurement, Monitoring and Environment Analysis, 2011-2015) and in a related study in Finnish Metrology Centre MIKES (nowadays a part of VTT). These studies are related to the development of a realtime SO<sub>3</sub> optical spectrometer (Hieta 2014) and a SO<sub>3</sub>-calibration unit (A. Wemberg 2014). A thermodynamic study on the phase equilibrium of SO<sub>3</sub> - H<sub>2</sub>SO<sub>4</sub> system in water containing flue gas matrix defined the proportion of SO<sub>3</sub> as a function of temperature and water contents (Pyykönen 2010). The study shows that at 5 % water contents H<sub>2</sub>SO<sub>4</sub> is the dominant component below 300 °C and at 10 % water contents about 10 % of SO<sub>3</sub> is converted to H<sub>2</sub>SO<sub>4</sub> at 400 °C. This leads to the requirement that direct SO<sub>3</sub> measurement should be carried out preferably at over 400 °C temperatures. High temperatures with reactive gases such as SO<sub>3</sub> make high demands on the durability of optical connections and gas cells but by using inert materials and protection gas optical connections, these issues could be circumvented.

Hieta et al. describe the development of an optical SO<sub>3</sub> analyzer (Hieta 2014) based on quantum cascade laser operating in spectral region between 1390 - 1400 cm<sup>-1</sup> or about 7.16 μm. The study showed that in this IR-region it is necessary to operate at low pressure as pressure induced line broadening makes the spectral features a continuum at ambient pressures. This means that this optical method is only applicable as an extractive method, and a cross-duct measurement is not

possible. The developed system measures simultaneously  $\text{SO}_2$  (limit of detection LOD 0.13 ppm),  $\text{SO}_3$  (LOD 0,007 ppm) and  $\text{H}_2\text{O}$ .

In a dissertation study (Vainio 2014) several extractive indirect methods for  $\text{SO}_3/\text{H}_2\text{SO}_4$  analysis were compared in laboratory and in process conditions. It was shown that some of the methods could be reliably utilized in  $\text{SO}_3/\text{H}_2\text{SO}_4$  analysis in biomass boiler studies (Vainio 2014). These methods are useful if continuous monitoring e.g. for the control of  $\text{SO}_3$  contents is not required. In this approach extracted gaseous  $\text{SO}_3/\text{H}_2\text{SO}_4$  is fed through a teflon tube packed with salt such as NaCl, KCl,  $\text{K}_2\text{CO}_3$  or  $\text{CaCl}_2$ . In normal operation mode, the salt is dissolved to water after the sampling and analyzed for sulphate ions. Especially salt methods with NaCl and KCl were observed to give reliable results without any significant interference with  $\text{SO}_2$ .

In this study a continuous extractive method for  $\text{SO}_3/\text{H}_2\text{SO}_4$  analysis was also tested for process control applications (Vainio 2014). In this approach, extracted gaseous  $\text{SO}_3/\text{H}_2\text{SO}_4$  is fed through a teflon tube packed with KCl. HCl is released in the sulphation reaction of KCl, and the sulphate concentration is determined by measuring HCl with FTIR method. The results indicate that it is possible to quantify  $\text{H}_2\text{SO}_4$  concentration by HCl concentration. However, this approach contains some uncertainties related to oscillations between the reaction products  $\text{KHSO}_4$  and  $\text{K}_2\text{SO}_4$  and the development of the method was left to further studies (Vainio 2014).

In a report of The Danish Environmental Protection Agency (Fateev and Clausen 2016), a system with cross-stack FTIR measurement capability (resolution  $0.25 \text{ cm}^{-1}$ ) was tested in laboratory and in a power station. In laboratory tests the system was calibrated with a high temperature flow gas cell for cross-stack and emission measurements by using the standard controlled condensation method. Field experiments were carried out in two stacks with 4 m and 14 m path lengths. In field experiments with high and low sulphur contents of fuel there was no difference in spectral responses. This was considered to mean same concentrations of  $\text{SO}_3$  for both fuels, but large difference in  $\text{SO}_2$  did not support this view. Also the  $\text{SO}_3$  concentration could have been very low or less than the LOD of the system or few ppm. The capture of  $\text{SO}_3$  to ash particles was speculated as an explanation. Interference between fly ash and  $\text{SO}_3$  has been considered e.g. in coal-fired boilers (Cao 2010). Another experiment at a different block showed that it was not possible to carry out a cross-stack measurement as the visibility through the flue gas (length 14 m) was too low. In this case an emission measurement was tested instead of cross-stack measurement. Here the LOD for  $\text{SO}_3$  was estimated to be 15 ppm for about 15 min measurement time.

There are few manufacturers which offer direct or indirect  $\text{SO}_3/\text{H}_2\text{SO}_4$  measurement systems for various process applications. The main application of these monitoring systems is their use in the control of  $\text{SO}_3$  by chemical injection in power plants. This makes possible to prevent corrosion caused by  $\text{H}_2\text{SO}_4$  in plant hardware. Moreover,  $\text{SO}_3$  monitoring can be used also for the improving

ESP performance in plants where fly ash contains high amount of alkali (Srivastava 2002). Direct  $\text{SO}_3$  analyzers are offered by ThermoFisher Scientific Inc. (Arke  $\text{SO}_3$  System) (Thermo-Fisher 2018) and CEMTEK Instruments Inc. (CEMGAS 5000) (CEMTEK Instruments 2018). Both of these direct  $\text{SO}_3$  measurement systems use extractive sampling, laser light source and low pressure optical cell.

An example of an indirect continuous measurement system is given by Pentol GmbH (Pentol  $\text{SO}_3$  online monitor) (Pentol 2018). In Pentol monitor, gas sample is first diluted with isopropanol + water mixture. Then, after reaction with bariumchloranilate, a color change is monitored with a photometer which gives a signal proportional to  $\text{SO}_3$  concentration. Pentol  $\text{SO}_3$  online monitor seems to be an automated version of the standardized isopropanol absorption bottle method described in EPA Method 8 (EPA 2018).

Cordtz et al. (Cordtz 2013) describe an automated and continuous analysis of  $\text{SO}_3$  with Pentol  $\text{SO}_3$  (Pentol GmbH) analyzer connected to the exhaust channel of an 80 kW medium-speed test engine. The engine is driven with different injection timing, engine loads and fuel input to find out the effects to the formation of  $\text{SO}_3$ . There seems to be lack of comparison data on accuracy and repeatability of Pentol  $\text{SO}_3$  system. Cordtz et al mention only one report on the comparison with the widely used controlled condensation (CCD) method with no significant differences. In a recent article, Zheng et al. report on the development of an automated continuous monitor for  $\text{SO}_3$  measurements which utilize isopropanol absorption and spectrophotometric determination. Their analysis on existing  $\text{SO}_3$  monitoring methods points out the possible interferences with  $\text{SO}_2$ , PM and moisture. In a field evaluation test the method was compared with CCD showing less than 2% differences at inlet and outlet of ESP (Zheng 2017).

According to a recent conference abstract Chien et al. (Chien 2017) examine two technologies for direct  $\text{SO}_3$  monitoring, namely differential optical absorption spectroscopy DOAS and external cavity quantum cascade laser EC-QCL. Unfortunately, final report is not yet available.

## 4 Measurement campaigns and methodology

### 4.1 Description of work

Within the project a number of laboratory and field measurement campaigns were performed:

- At VTT's laboratory PM and NH<sub>3</sub> verification measurements were performed with diesel bus
- At VTT's laboratory numerous NH<sub>3</sub> measurements were performed on sensor test bench with natural gas engine.
- The field measurements included
  - Two NH<sub>3</sub> sensor long-term trials on ships
  - PN and NH<sub>3</sub> sensor study on-board ships in two measurement campaigns in co-operation with the other projects. Also PM filter materials were studied.
  - A DF marine engine measurements for studying the PN and PM emissions and performance of the measurement methods (Pegasor PPS, PM filter materials).
- At VTT's laboratory, methane catalyst was studied (regeneration procedure for catalyst materials).

Testing of potential sensor systems for gas and particle monitoring requires realistic environments and long-term testing which is often very difficult to arrange in laboratory conditions. This is why we have used months' long tests in cruising ships to see the real applicability of measurement systems besides shorter on-board testing periods where an extensive set of instrumentation was used to verify the results.

One of the most important aspects in our way of working in this subproject is the utilization of opportunities offered by other ongoing projects at VTT. For example, the arrangement of ship measurement campaigns requires a lot of work and careful planning long before the intended campaign, but it also offers versatile information and comparison data from other research groups.

In this work, the Hercules-2 project took part to the on-board measurement campaigns organised by the SEA-EFFECTS BC (<http://www.vtt.fi/sites/sea-effects>) and EnviSuM (<https://blogit.utu.fi/envisum/>) projects. Both measurement campaigns were conducted by VTT Technical Research Centre of Finland, Finnish Meteorological Institute and Tampere University of Technology. The financial support for the SEA-EFFECTS BC project was received from Tekes (40356/14), Trafi (172834/16) and from industrial partners, Wärtsilä, Pegasor, Spectral Engines, Gasmot, VG-Shipping, HaminaKotka Satama Oy, Oiltanking Finland Oy and Kine Robotics, and for the VTT's contribution in the EnviSuM project from Trafi (58942/17).

Hercules-2 project covered the development of the following methods used in the on-board campaigns:

- PN measurements
- NH<sub>3</sub> sensor measurements
- Development of small size PM sampling system for on-board measurements

In the laboratory work and in the field tests, VTT's Engine and vehicle laboratory's 20 years' experience of performing emission measurements with wide variety of engine and vehicle technologies, fuels, engine oils and aftertreatment systems were utilised. In total, VTT's facilities comprise the following basic set-up for engine and vehicle research:

- Wärtsilä Vasa 4L32, 1640 kW medium-speed engine.
- Five dynamometers for high-speed engines.
- Chassis dynamometer for heavy-duty vehicles
- Chassis dynamometer for light-duty vehicles.
- Besides research in laboratory, we measure at site and on-board ships.



In the Hercules project, methane oxidation catalyst was studied at VTT's engine laboratory. Catalyst test benches are in significant role in our facilities for the research of emission abatement technologies and fuels. We have catalyst test benches equipped with a versatile selection of gas and particle measurement systems such as FTIR, LDS, MicroGC, and sampling systems developed for SCR units. The facilities include also standard PM measurement systems, and instruments such as ELPI and CPC for particle size distribution and number determination with predefined cut-off limit. In this project we have utilized VTT's catalyst test bench and measurement facilities for gas and diesel engines (Figure 3).

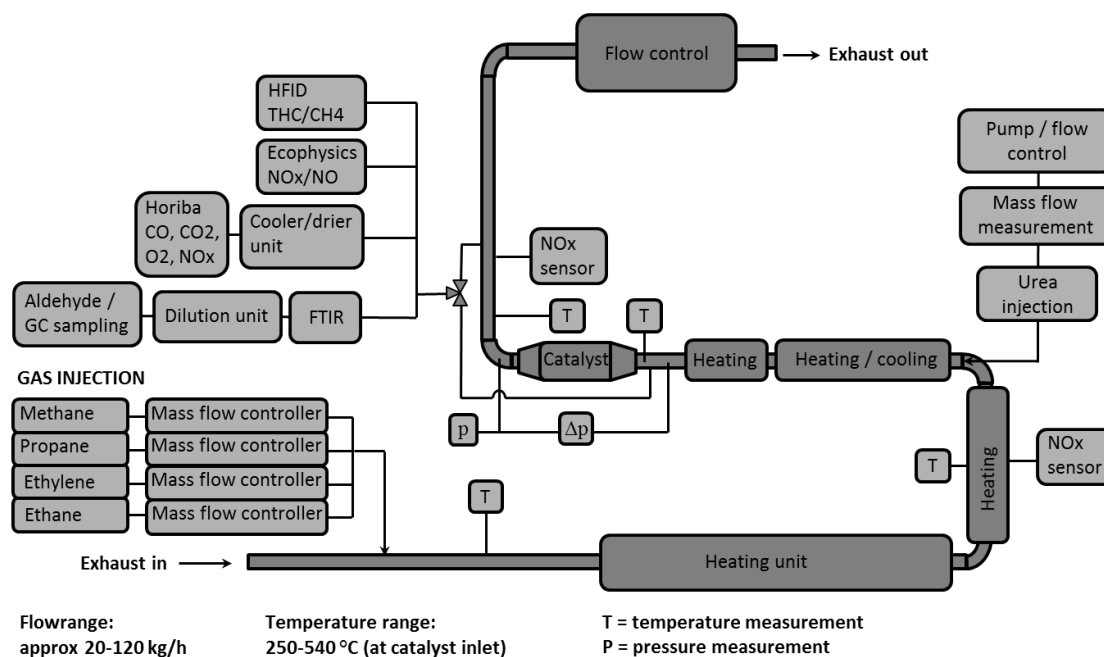


Figure 3. Catalyst test bench at VTT.

Exhaust emissions can be characterized extensively in detail both in laboratory and field measurements at VTT (Table 1). Various gaseous emission components can be analysed using real-time techniques. Several methodologies are available for measuring PM and PN emissions. Also a number of other advanced analyses, such as particle numbers and sizes, compositional analyses of PM (anions, metals etc.) and morphological characterization are available.

Strength at VTT is capability to use existing analysis methods in difficult conditions, for example in the on-board measurements, and to develop new testing facilities and measurement devices for the needs of each project. Understanding different exhaust sources in relationship with the fuels, engine oils and emission control technologies used help in designing the suitable test set-up for different purposes (e.g. probes, diluters, equipment).

Besides the results and methods included in this report, on-board measurements that were conducted in co-operation with the SEA-EFFECT BC and EnviSuM projects covered a comprehensive set of measurements listed in Table 1 and beyond, for example black carbon (FSN, MSS, MAAP, Aethalometer, SP-AMS), gaseous emissions and particulate matter properties (concentration, size distribution, optical properties, secondary aerosol formation potential). These results have been reported within the above-mentioned projects (Timonen et al. 2017, Teinilä et al. 2018). In addition to the measurements by VTT, extensive in-depth characterisation of exhaust was conducted by FMI and TUT in the SEA-EFFECT BC and EnviSuM projects. Most of the instruments were online instruments with a good time resolution. Also in-depth chemical analysis from filter samples are available.

*Table 1. VTT's portfolio of exhaust emission measurements.*

<b>Gaseous emissions:</b>	<b>Composition and quality of PM and SVOC</b>
<ul style="list-style-type: none"> <li>• CO, HC, NO<sub>x</sub>, CO<sub>2</sub></li> <li>• NO<sub>2</sub>, N<sub>2</sub>O</li> <li>• Ammonia (NH<sub>3</sub>)</li> <li>• Sulphur oxides (SO<sub>x</sub>)</li> <li>• Aldehydes and alcohols</li> <li>• Speciated hydrocarbons</li> <li>• Siloxanes, supertoxics</li> </ul>	<ul style="list-style-type: none"> <li>• Elemental and organic carbon (EC/OC)</li> <li>• Black carbon (FSN)</li> <li>• Volatile condensables</li> <li>• Sulphates, nitrates and other anions</li> <li>• Polyaromatic hydrocarbons (PAH)</li> <li>• Biological analysis (Ames, DTT)</li> <li>• Metals</li> </ul>
<b>Particle mass (PM) and semivolatile (SVOC) sampling</b> <ul style="list-style-type: none"> <li>• Dilution with full and partial flow tunnels, ejectors, porous tube diluters, thermodenuder for volatility</li> <li>• Hot stack sampling</li> <li>• Several filter materials and sizes available</li> </ul>	<ul style="list-style-type: none"> <li>• Carbon, nitrogen, oxygen, hydrogen, sulphur</li> </ul> <b>Mass, number and size classification of particles, special characterisation</b> <ul style="list-style-type: none"> <li>• Mass size classification: DLPI, DGI, virtual impactors (PM 2.5 and PM1)</li> <li>• Number size classification: ELPs, CPC</li> <li>• Morphology analysis using SEM and TEM electron microscopes</li> <li>• Chemical characterization using FTIR microscopy for solids</li> </ul>

VTT is accredited by Finnish accreditation body FINAS as the accredited testing laboratory T259, accreditation requirement SFS-EN ISO/IEC 17025 (FINAS 2018). Accreditation includes among other methods the PM measurement in laboratory according to ISO 8178-1:2006 and NH<sub>3</sub> measurement with FTIR according to SFS 5624 and Technical Guidance Note M22. In the measurement campaigns of this project the best practices of ISO 8178-1:2006 have been utilized, but the measurements cannot be considered as accredited measurements.

## **4.2 Particulate matter and particle number studies**

### **4.2.1 PM measurement methods**

#### **4.2.1.1 Principle of PM measurement (ISO 8178)**

PM emissions were measured according to ISO 8178-1:2006 standard. In 2017 a new version of the standard was introduced (ISO 8178-1:2017). New version includes more strict specifications for PM measurement and includes requirements for PN measurement. The PN measurements for this project are performed according to year to the latest version of the standard.

PM measurement of large engines is based on a partial-flow dilution of the exhaust gas. Standard describes multiple possible solutions for partial-flow dilution systems. However, the basic principle of the all partial flow systems is that part of the exhaust gas flow is extracted to a dilution tunnel in



which clean dilution air is mixed with the exhaust gas. Then the mixture or part of the mixture is lead through a sampling filter on which the particles are collected. Sampling filter is weighted before and after the test and the difference between weighted masses is the mass of particle material collected from the sample flow. The main parts of the sampling system are sampling probe, transfer tube, dilution tunnel, sample filter holder, flow control for dilution air and sample flow and pump (Figure 4).

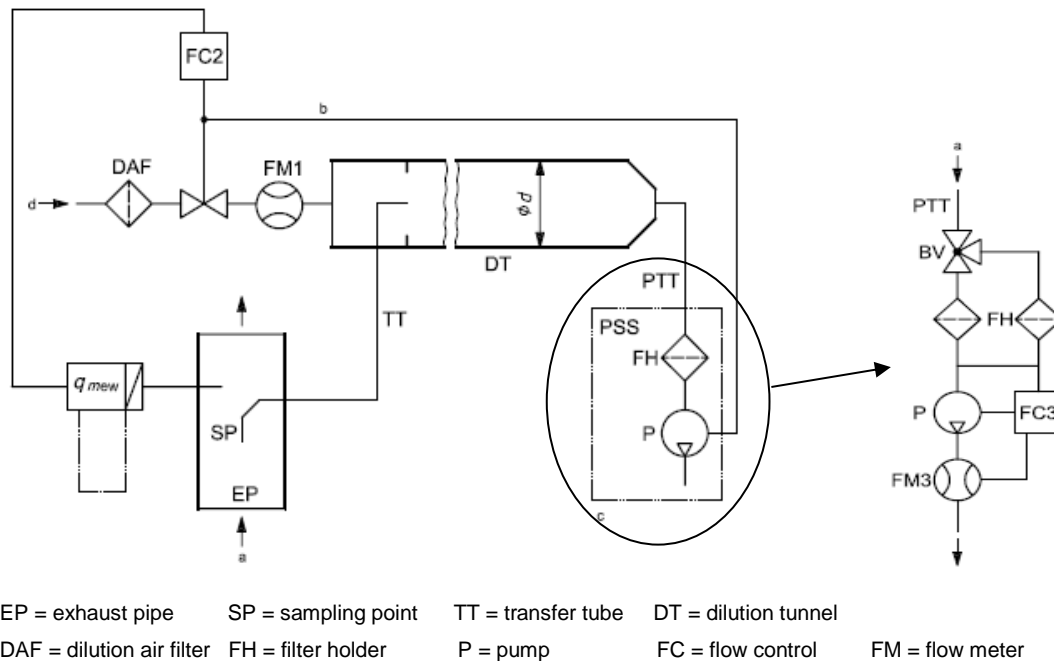


Figure 4. Partial-flow dilution system with flow control and total sampling. (ISO 8178-1:2006)

The main specifications of the system according to 8178-1:2006:

- Transfer tube
  - o isolated if length < 1 m
  - o heated to wall temperature of 250 °C if length 1-5 m
  - o maximum length 5 m
  - o inside diameter equal or greater than sampling probe diameter but less than 25 mm
- Dilution tunnel
  - o minimum diameter for total-sampling type 25 mm
  - o must ensure complete dilution air and exhaust gas mixing within the tunnel length
  - o can be heated up to wall temperature of 52 °C
- Dilution air
  - o filtered, dehumidification is allowed
  - o temperature between 15 to 52 °C
- Condition at sampling filter
  - o face velocity 30-100 cm/s
  - o Temperature 42 - 52 °C

- Sampling filter
  - o minimum filter size 47 mm
  - o Filter material: fluorocarbon coated glass-fibre filters or fluorocarbon membrane filters

The list above is not comprehensive. The standard includes various other requirements for PM sampling device and e.g. for filter weighing. The current requirements needs to be checked from the latest version ISO 8178-1:2017.

#### 4.2.1.2 Commercial AVL 472 Smart Sampler

VTT uses AVL 472 Smart Sampler for partial-flow PM sampling. Smart Sampler is partial-flow dilution system with flow control and total sampling type of device as described in ISO 8178-1:2006. Instrument consist of two units, the filter holder unit and flow control unit, which also includes all the needed electronics (Figure 5). The flow control of the system is based on two mass flow meters, which control the dilution air flow and sample flow through sample filter. It is crucial that the mass flow meter readings are accurate and therefore the mass flow meters are placed in a heated box for stabilizing the operating temperature. System also have internal laminar flow element which is used for mass flow meter checks on daily basis and if needed the mass flow meters are re-calibrated with the control software of the device. Since the ISO 8178-1:2006 included new requirement for filter holder temperature, the original filter holder unit was modified at VTT and the filter holders and dilution tunnel were placed inside a heated cabin (Figure 5).

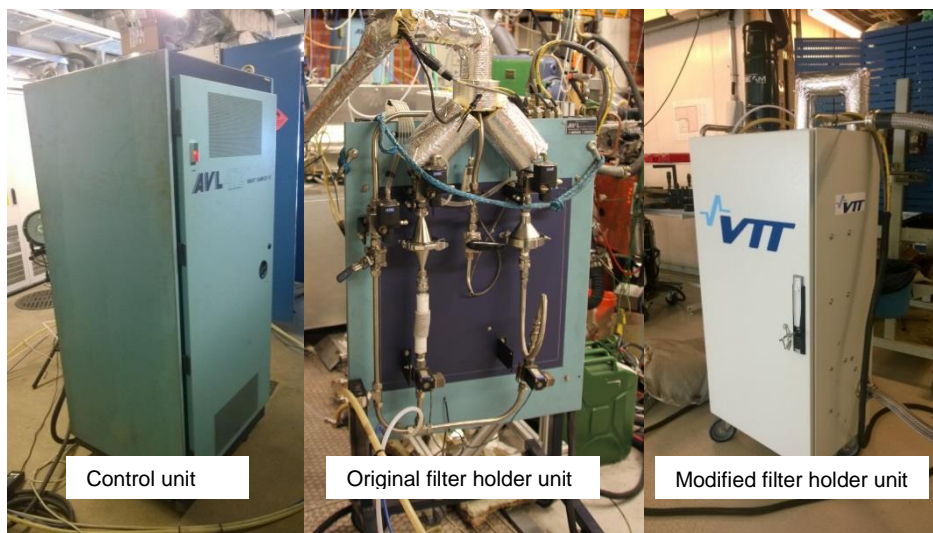


Figure 5. VTT's AVL 472 Smart Sampler.

#### 4.2.1.3 VTT's in-house movable Ship Dilution System (PM-SDS)

AVL instrument is large and heavy (Control unit 73 x 64 x 164 cm, 245 kg and dilution unit 75 x 56 x 153 cm, 60kg) and therefore not very suitable for all field measurements. At VTT, a small movable

Ship Dilution System (PM-SDS) was designed and built-up in the Hercules-2 project. PM-SDS uses the same measurement principle as AVL Smart Sampler. It has flow controllers for dilution air and sample flow. Flow controllers and control electronics are placed in a small cabinet. For maintaining a constant temperature for mass flow controllers the cabinet is heated. The dilution tunnel is a porous tube diluter designed at VTT. The diluter and filter holder is placed in a second portable cabinet, which also includes heater for the dilution air. The sample temperature at the sample filter is controlled with dilution air temperature. Third part of the system is a portable vacuum pump (Figure 6 and Figure 7). The system is capable to sample flows up to 1.3 g/s, which equals 98 cm/s filter face velocity at 47 °C when using 47 mm sample filter. The size for the sampling unit is 60 x 40 x 25 cm and for the control unit 86 x 60 x 43 cm. Weights for the units are ca. 20 kg (sampling unit), 30 kg (control unit) and 10 kg (pump).

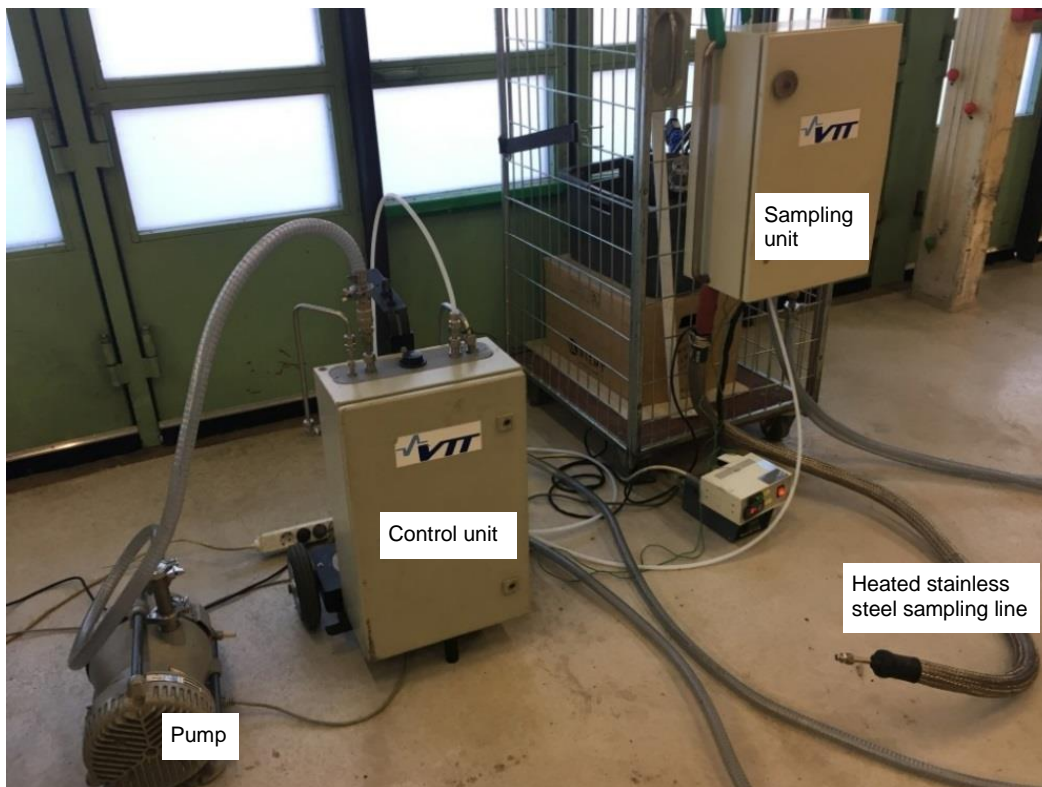


Figure 6. VTT's PM-SDS sampling system assembled in laboratory.

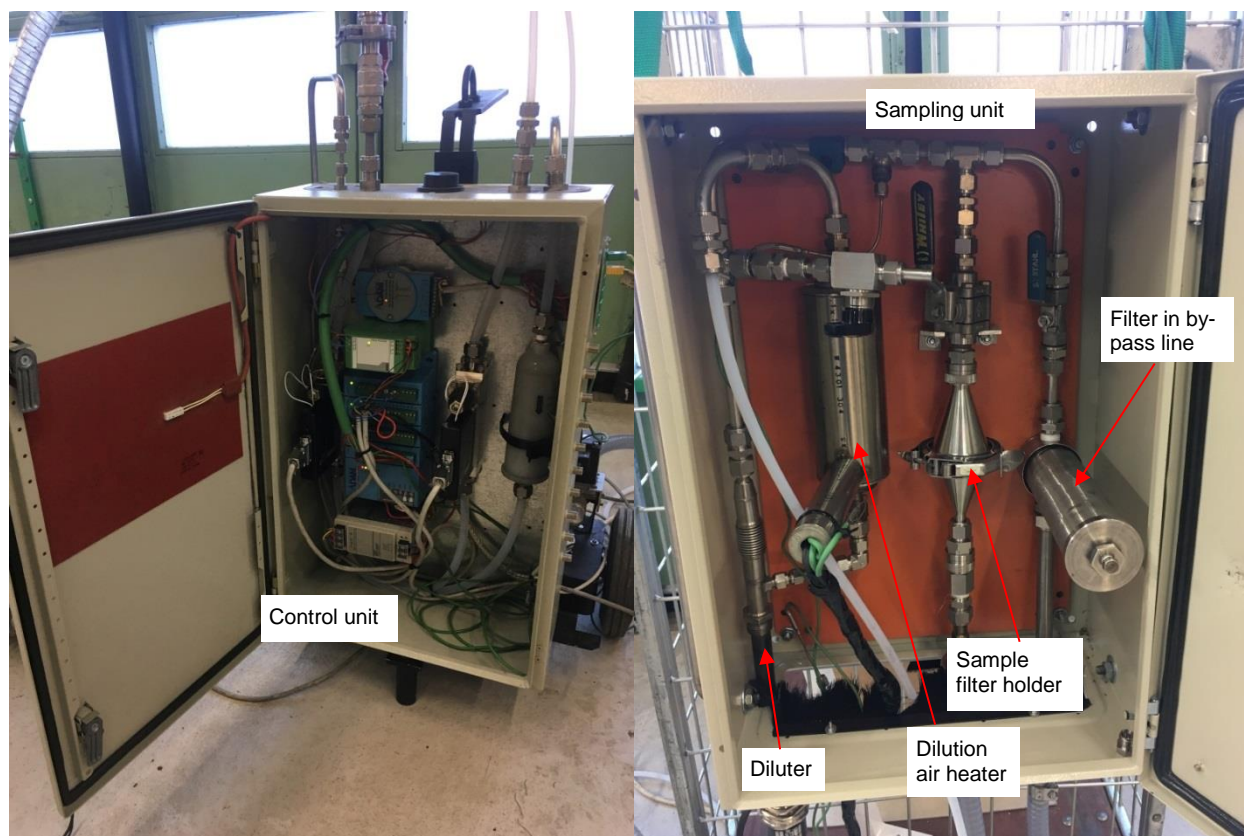


Figure 7. Control and sampling unit details.

Before field measurements the PM-SDS flow controllers are calibrated at the laboratory with laminar flow element flow calibrator. During the field measurements a daily flow checks of the sample inlet flow are performed with flow calibrator based on the principle of positive displacement. Calibration set-up used in field conditions is described in Figure 8.

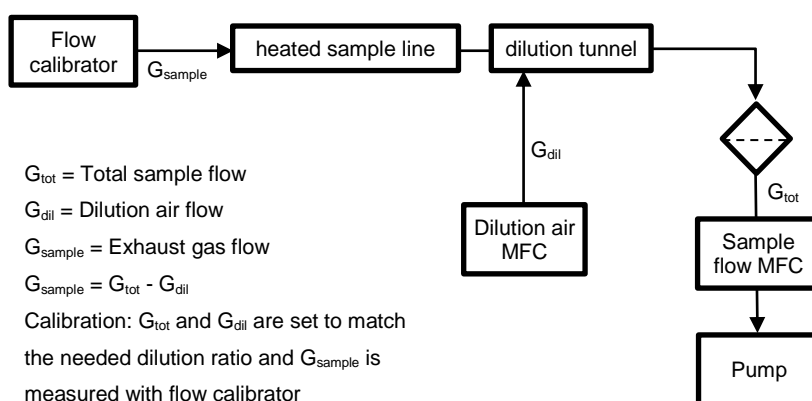


Figure 8. Flow calibration set-up of PM-SDS on field conditions.

In this project, the field measurements were performed using dilution ratio (DR) 10 and filter face velocity in different campaigns varied from 74 to 99 cm/s. Sample filters had 47 mm diameter and filters were PTFE coated glass fibre filters (Pallflew TX40-HI20WW). For the on board

measurements PM was collected using primary and back-up filters, the other measurements were carried out using only primary filter. A heated transfer line (250 °C) was used in all measurements, the length of the transfer line varied from 2 to 6 meters. Transfer line used in measurement on ship B was longer than accepted in ISO 8178 but on that case (Chapter 3.1.5) it was not possible to use shorter line.

#### **4.2.1.4 Filters studied in PM collections**

Different filter materials were studied on-board ship B and with Dual-Fuel marine engine. ISO 8178 PM sampling is typical in Europe using PTFE bonded glass fiber filters, while US EPA requires use of PTFE filters. We studied PM sampling from marine engine E3 using the four types of filter materials, two PTFE-types, one PTFE bonded glass fiber and one quartz quality filters:

- Pallflex TX40HI20-WW, o.d. 47 mm. Filter material is borosilicate microfibers reinforced with woven glass fibre coated with cloth and bonded with polytetrafluoroethene (PTFE, Teflon). Both primary and back-up filters were used. This filter type is common in Europe for PM measurements.
- Pallflex Teflo 2, o.d. 47 mm, PTFE reinforced with polymethylpentene (PMP). Typical thickness 46 µm (516-8912, VWR), 2 µm porosity. Flow 53 l/min/cm<sup>2</sup> (0.7 bar). Back-up filters were not used. PTFE filters are used in USA for PM measurements.
- Whatman PM2.5 PTFE. O.d. 46.2 mm, 2 µm porosity. Back-up filters were not used. Meet EPA PM2.5 requirements (40 CFR Part 50, Appendix L). PTFE filters are used in USA for PM measurements.
- Tissuquarz 2500QAT-UP, o.d. 47 mm. A pure quartz without binder. The quartz filters were pre-cleaned at 850 °C for two hours and stabilized. The back-up filters were not used in the collections with quartz filters. Quartz filters are used for EC/OC and metal analyses.

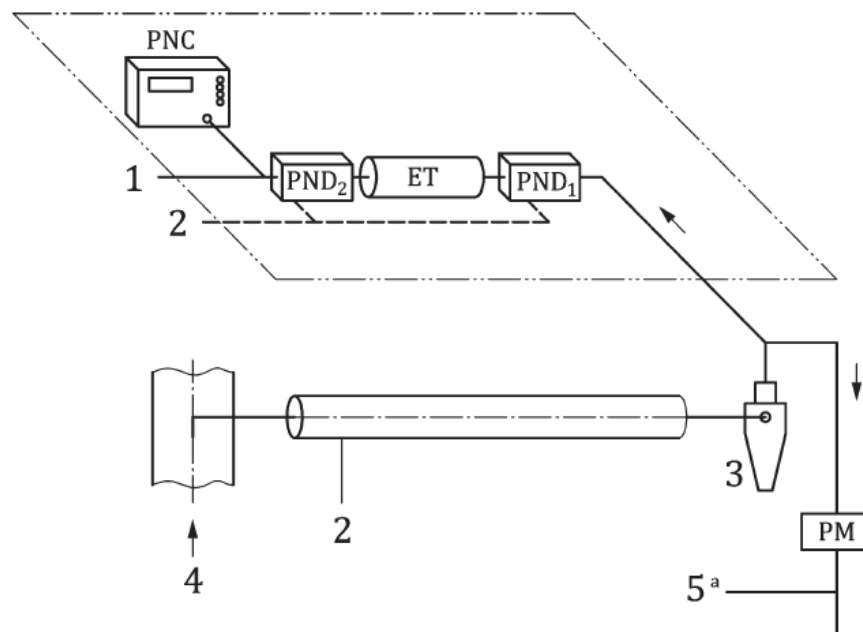
With dual-fuel marine engine, the studied filters were the same as with engine E3 with an exception of quartz filter, which was left out from the study.

## **4.2.2 PN measurement methods**

### **4.2.2.1 Principle of PN measurement**

PN measurement method for certification purposes of light duty vehicles was firstly introduced in UNECE Regulation 83 on 2009 (UNECE 2018). Later, the method was adopted in European legislation to heavy-duty engine verification and will be adopted on 2019-2020 to non-road mobile machinery including inland waterway vessels. As earlier mentioned the method is also included to ISO 8178-1:2017 standard. VTT has been using the method for vehicle measurements since 2014. Method is developed for measuring the number of solid particles in size class above 23 nm. Method includes sample precondition unit (volatile particle remover, VPR) and particle number counter

(PNC). Figure 9 presents the schematic drawing of a typical partial-flow sampling system described in ISO 8178-1:2017. The PN measurement system is combined with PM measurement system. The sample after the dilution tunnel and cyclone (cyclone is recommended not mandatory) is divided to PN and PM measurement devices. Since the PM system typically controls the flows and DR, the flow removed by the PN system must be compensated with external air flow or by the controlling software.



#### Key

- |   |              |   |   |
|---|--------------|---|---|
| 1 | excess air   | 4 | from engine exhaust   |
| 2 | filtered air | 5 | make-up air   |
| 3 | cyclone      | a | Alternatively, the control software might account for the flow removed by the PN system |

Figure 9. Typical partial-flow sampling system for PN measurement (ISO 8178-1:2017).

VPR consist of primary and secondary diluters (PND1 and PND2) and evaporation tube (ET) in between diluters. It is also possible to use additional dilution after the ET to get the PN concentration suitable for PNC. The dilution factors of the diluters are defined in regulations. For the VPR there is no definition for total dilution factor. Instead of that Particle Removal Factor (PRF) must be defined for the VPR. PRF includes the effect of dilution factors of PNDs and also particle losses of the VPR. Some main parameters for the system are listed below.

Some main specifications of the PN measurements system required by ISO 8178-1:2017:

- PND1
  - o Wall temperature 150 - 400 °C
  - o DR 10-200
- Evaporation tube wall temperature 300 - 400 °C and greater or equal than in PND1
- PND2 DR 10-15
- HEPA filtered dilution air must be used
- Particle concentration after VPR less than the upper threshold of the single particle count mode of the PNC
- Sample gas temperature at PNC inlet < 35 °C
- PNC counting efficiencies 50% at 23 nm and >90% at 40 nm

#### 4.2.2.2 VTT's PN measurement system

VTT has two identical measurement systems for measuring PN according to UNECE Regulation 83 and 49. VTT uses combination of Dekati DEED (VPR) and Airmodus A23 CPC (PNC). Dekati DEED has two selection for PRF which are 100 and 1000. When measuring diesel engines without DPF it is often needed to have a higher PRF for achieving low enough particle concentration for the PNC. Figure 10 presents the measurement set up for PN measurements in this project. The sample for the PN system has been taken from the AVL Smart Sampler. The dilution factor for Smart Sampler has been 10. The flow taken from AVL Smart Sampler has been compensated with external flow feed for avoiding incorrect function of the Smart Sampler's flow control system.

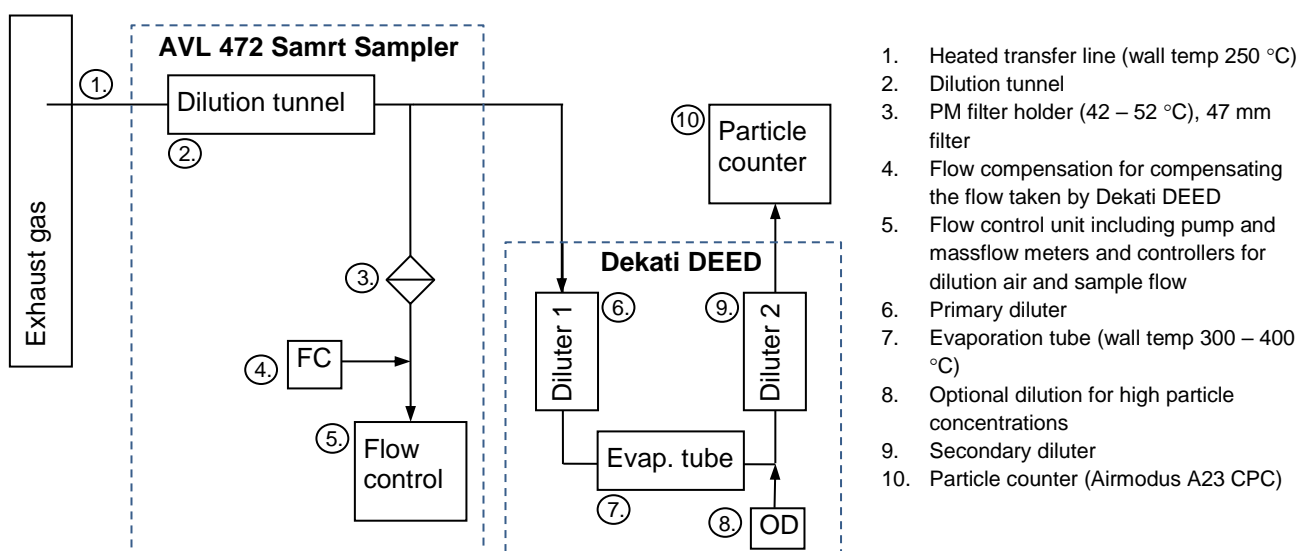


Figure 10. VTT's PM and PN measurement set-up.

#### 4.2.2.3 Diffuse charging sensor, Pegasor PPS-M

Pegasor's PPS-M particle monitor was selected for comparison tests in the field measurements of workpackage 7.4. The selection is based on its capability to particle mass and number concentration monitoring, fast response and it could possibly become a cost-effective solution for on board diagnostic (OBD) systems. PPS-M represents the diffuse charging sensor type and it gives a signal which is primarily proportional to the surface area density of the particle flux. The signal is obtained by measuring the so-called escaping current which is the current carried out by particles escaping from the charger unit (Rostedt 2014) (Ntziachristos 2011). This signal can be calibrated to PM and PN densities which depend on the particle size distribution. According to the manufacturer, PPS-M sensor is designed for engine and after-treatment development, portable applications, stack monitoring and indoor and outdoor air quality monitoring. The flow-through principle makes possible a continuous and maintenance-free operation (Pegasor 2018).

A comparison test on two versions of PPS-M particle sensor, a versatile list of references, and a detailed discussion on its operational principle can be found in the dissertation study of Marc Besch (Besch 2016). The experiments are carried out in engine dynamometer, in chassis dynamometer and in on-road conditions. Besch notes that general properties of PPS-M make this sensor more attractive in OBD application than other sensor technologies. These properties include real-time measurement and sensor's response which is proportional to active surface area of particles.

The sensor's correlation coefficient with trends observed for CPC total particle concentration and gravimetric total particulate matter mass measurements are as follows: for TPM:  $R^2 = 0.953$ , and for CPC:  $R^2 = 0.983$  (Besch 2016). The sensor was observed to correlate better with total particle concentrations calculated from integration of particle size specific EEPS (EEPS gives the size distribution of engine exhaust particle emissions from 5.6 to 560 nm with fast time resolution) data as opposed to the total particle concentration measured with the CPC. This is explained by a smaller cut-off limit of CPC (2-3 nm) whereas PPS-M removes particles below about 18 nm. The other difference is the measurement principle: EEPS and PPS-M are similar concerning particle charging but, on the other hand, CPC is based on particle growth by a hydrocarbon and optical counting of these larger particles.

These differences are indicated by a multi-day comparison test with different fuels. The test showed that PPS-M total particle number concentration correlates well the trends in EEPS and CPC data. However, there is a systematic difference between the CPC measurement and the EEPS and PPS-M measurements by a factor 2.5-2.7. The same test shows that PPS-M results are within 1.9% to 18.9% in comparison with EEPS data (Besch 2016).

Short term stability of the sensor was studied in a repeatability test. The test was carried out in engine dynamometer and it showed that the sensor's average coefficient of variation (the ratio of



the signal's standard deviation  $\sigma$  to the mean  $\mu$  in %) was < 2% with different steady-state and transient cycles (Besch 2016).

The applicability of PPS-M sensor as a monitor of damaged diesel particulate filter (DPF) in OBD system was tested against AVL Smokemeter 415S in an engine dynamometer and in vehicle in driving cycle test (NEDC) (Ntziachristos 2011). The report concludes that the maximum theoretical error is 18% when using surface area information for particle number density, and 30% when surface area information is used for particle mass density. The error is expected to be much lower if the sensor is calibrated for the particular engine or vehicle. In NEDC test, the sensor could repeatedly distinguish a damaged DPF with 6 mg/km emission level from a functional DPF with 1 mg/km emission level.

In a recent article, a new dPPS concept has been introduced to circumvent the dependency of PN and PM results on the particle size distribution of PPS-M (Amanatidis 2016). A dPPS device is capable to measure mean particle size, and by this information improved estimates to PN and PM can be given (Amanatidis 2017). A dPPS device can also divide particles to different size classes e.g. to cut off particles under 23 nm as required by EU standards for PN measurement. The test with dPPS shows that dPPS is an appropriate candidate as a portable emissions measurement system (PEMS) to measure both particle mass and number exhaust emissions. Correlation between the APC reference instrument used in the study and a dSSP sensor gave the correlation coefficient  $R^2=0,82$  for PN, and  $R^2=0,97$  for PM (Amanatidis 2017).

There are several other particle sensor technologies dedicated to OBD application. In an on-going project (Khalek 2017) the following technologies were selected for tests: electric resistance cumulative sensor, real time sensor based on the use of natural charge of particles, and sensor based on current measurement from particles charged with corona discharge. According to the report sensors show some promising results, and there has been significant progress in sensors' compliance with OBD requirements. Unfortunately, the final report is not yet available.

In this project Pegasor PPS-M sensor was used in the measurements of dual-fuel marine engine. Sensor was provided for the measurements by Pegasor and Pegasor's personnel used the sensor in the measurements. The sensor set-up is presented in Figure 11. sample flow to sensor is ca. 2.6 l/min. The exhaust gas diluted with heated dilution air (180 °C) before the sample line which is also heated to 180 °C. Before the sensor the precharger removes ions and charged particles with negative diffusion charger. At this point the sample gas is also diluted with small amount of dilution air. The total dilution factor before the sensor is 2. After the precharger the sample goes to sensor which is heated up to 200 °C. The diluted exhaust gas is then returned to the exhaust pipe.

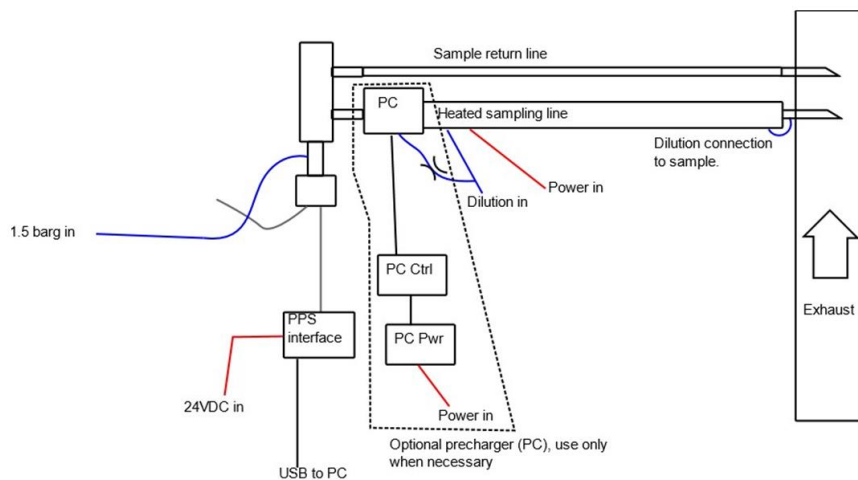


Figure 11. Pegasor PPS-M sensor set-up in the dual-fuel marine engine measurements (Pegasor)

### 4.2.3 Measurement campaigns

#### 4.2.3.1 Laboratory verification of VTT's movable SDS-PM system

As described in Chapter 4.2.1.3 a small size movable PM-SDS was build-up at VTT for on-board and other field measurements. For verifying the PM-SDS, a comparison measurement at VTT's Engine and vehicle laboratory was performed using AVL Smart Sampler and PM-SDS (Figure 12 and Figure 13). Figures clearly show the size difference the Smart Sampler and PM-SDS. A Euro II emission level diesel truck was used as a "particle generator" for the measurements on heavy-duty chassis dynamometer. Truck was driven on constant speed (85 km/h) for getting a stable PM emission. Comparison measurements were performed with four different DRs (5, 10, 15 and 20) and at least four repetitions with each DR were measured.

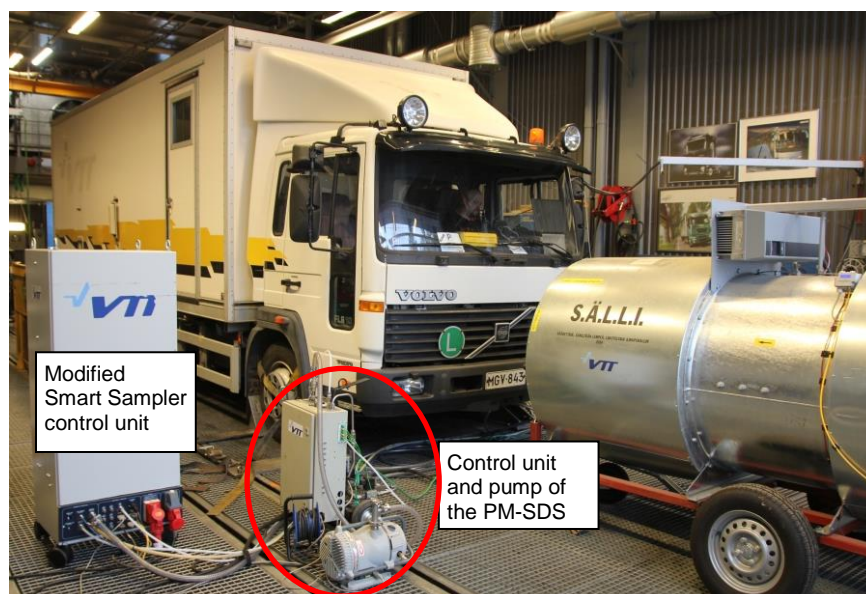


Figure 12. PM device installation on VTT's heavy-duty chassis dynamometer. The size difference of the devices is obvious.

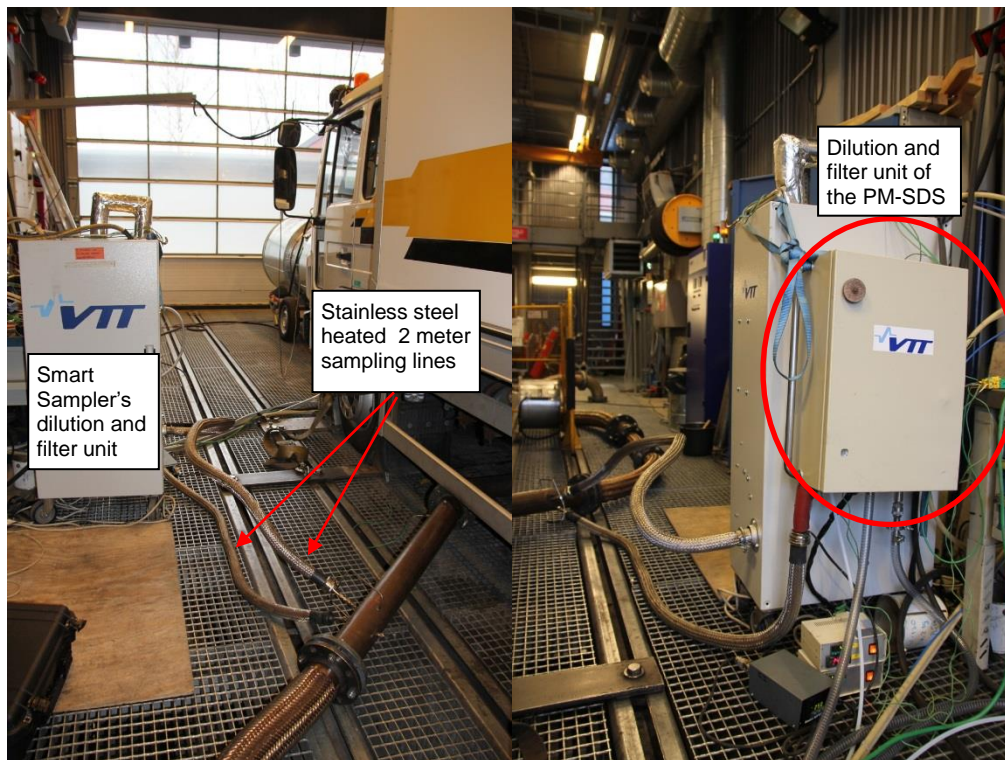


Figure 13. PM device installation on VTT's heavy-duty chassis dynamometer.

#### 4.2.3.2 Dual-fuel marine engine

VTT's PM and PN measurement set-up as described in Figure 10 was used for measurements with a modern DF marine engine. In addition to VTT's devices, Pegasor PPS-M particle sensor was also measuring the PN concentration. Engine was measured on DF and diesel operation modes using five different engine loads (100, 75, 50, 25, 10%). On each load 2-3 PM measurements were performed, PN emissions were measured and recorded with 1 Hz interval over during the measurements. Measurement campaign included also PM filter material comparison using 25% load and running the engine with LFO.

#### 4.2.3.3 On-board PM and PN studies

The two on-board measurement campaigns were as follows:

- a) **On-board a modern cruising ship (A) with a selective catalyst reduction (SCR) catalyst and a hybrid scrubber, 2016.** For the purposes of Hercules-2 project the PM and PN emissions from two main engines (E1, E2) were measured at constant engine loads of 40% and 75%. The measurements were performed with the set-up presented in Figure 10. For E1, the results are before and after scrubber, and for E2 also before and after SCR. In most measurements, HFO fuel with 0.65% sulphur content was used, and for one engine also MGO with below 0.10% sulphur content. SEA-EFFECTS BC (<http://www.vtt.fi/sites/sea-effects>) on-board results are reported by Timonen et al. (Timonen et al. 2017).

- b) **On-board a RoPax ship (B) equipped with DOC and a seawater scrubber, 2017.** PM and PN from one of its main engines (E3) were measured before and after emission control devices. The measurements were performed with the set-up presented in Figure 10 with the exception that AVL Smart Sampler was replaced with PM-SDS device. HFO fuel with 1.9% sulphur content was used and in limited tests fuel was MGO containing below 0.10% sulphur. Ship B operated normally and thus engine load varied during cruise, however, mainly at 63-66% load. Some data was achieved at ~17% engine load in ports. EnviSuM (<https://blogit.utu.fi/envisum/>) on-board results are reported by Teinilä et al. (Teinilä et al. 2018).

AVL 472 Smart Sampler dilution and sampling system for PM was used on ship A. On ship B the VTT's PM-SDS was used for the measurements. This system could be moved between the decks of ship B without aid. For PM measurements, usually three replicate tests were conducted in different locations. On ship B two PM samples were taken also without heating to assure that heating did not cause evaporation.

Results are presented in as mg/kWh. From ship A, necessary information was available from ship data to convert concentrations to the emissions (mass per kg fuel or per kWh). Instead, for ship B fuel consumption was not recorded from individual engines. Based on the theoretical fuel consumption of 170 g/kWh, measured exhaust carbon dioxide (CO<sub>2</sub>) concentrations and fuel composition, calculations of fuel consumption and exhaust flows were conducted for ship B, however, addressed with excess uncertainty.

In both campaigns, analysed properties of engine oil showed that concentrations of engine wear metals were relatively low and oil was in good condition.

Many lessons were learned during on-board campaigns as reported by Timonen et al. (Timonen et al. 2017). Organising the on-board measurement campaigns requires careful preparations starting at least 6-12 months prior to campaign. Discussions and pre-visits with the technical personnel from the ship were essential to resolve availability of needed resources and conditions in the ship (e.g. connections to instruments, safety issues, moving and locations for instruments, ambient conditions, power and UPS, pressurised air, need for crane, customs declaration, regulations for pressurised gas bottles). Particularly important is to have competent measurement crew on-board since conditions are challenging and measurements cannot be prolonged or repeated. Also skills to repair and calibrate instruments on-board are needed. Co-operation with the ship personnel is utmost important in order to adjust the measurement points and to know the current engine parameters. After the campaign it is important to obtain the ship data (used engines, engine loads, fuel consumptions etc. as a function of time) in order to properly calculate the results.

### **4.3 *NH<sub>3</sub> measurement studies***

The study on the applicability of NH<sub>3</sub> sensors for SCR units was started at VTT in a national MMEA research program (Measurement, Monitoring and Environmental Analysis, 2011-2015). A reliable and cost-effective electro-chemical sensor could be an ideal solution for the control of urea dosing in SCR units. For a comparison test we selected the only commercial sensor available at that time or Delphi NH<sub>3</sub> sensor. The sensor is designed for low sulphur fuels and its tolerance to marine fuels was not known. In the comparison test the sensor's response was observed to be linear in comparison with LDS and with FTIR results (Murtonen 2015). The LDS and FTIR methods are accepted for NH<sub>3</sub> measurement according to ISO 8178-1:2017. In the workpackage 7.4 we expanded the sensor tests to field measurements in cruising ships, to long-term tests and to tests with different marine fuels. In addition to measurements in marine applications the sensor performance in comparison to other devices was tested with heavy-duty diesel vehicle, since the sensor is designed for automotive applications. These field measurements were supported by various laboratory analyses in VTT's engine and catalyst test benches.

The principles of different types of NH<sub>3</sub> detection methods for environment, process and automotive applications are described e.g. in Timmer's report (Timmer 2005).

#### **4.3.1 NH<sub>3</sub> measurements methods**

##### **4.3.1.1 Fourier transformation infrared method**

FTIR analyzer is widely used for measuring multiple gaseous compounds in exhaust gas. Raw exhaust gas sample is drawn, filtered and conditioned to 180 °C before it enters to FTIR. FTIR is based on how the different gaseous compounds absorb infrared radiation. The light absorption for a certain wavelength range is defined by Fourier transform algorithm. FTIR analyzer can measure simultaneously dozens of compounds. The downside of the FTIR method is that compounds have cross-interferences which needs to be taken into account when analyzing the measured spectrum. Same analysis method cannot be used for different emission sources without inaccuracies in the results.

In this project FTIR method was mainly used for measuring NH<sub>3</sub> in multiple measurement campaigns. The FTIRs used were Gaset DX4000 and MKS 2030. The Gaset device is designed for field measurements and the MKS device is purely for laboratory use.

NH<sub>3</sub> measurements with extractive methods are challenging because NH<sub>3</sub> has tendency to adsorb to sampling lines and filters. Also, if SO<sub>2</sub> is present in the exhaust gas, ammonium sulphate formats in the sampling system and the NH<sub>3</sub> values measured by FTIR are underestimated. The effect of these challenges can be minimized by using as short as possible sampling lines and increasing the

sample flow. However, especially with high sulphur marine fuels the extractive measurement methods are troublesome\_(Antson, et al. 2014),\_(Lehtoranta, Vesala, et al. 2015)

#### 4.3.1.2 Laser Diode Spectrometer method

LDS analyzer is designed for measuring specified gas compound. LDS method can be used for measuring e.g. O<sub>2</sub>, HF, HCl, NH<sub>3</sub>, H<sub>2</sub>O, CO, CO<sub>2</sub>. Measurement principle is based on single-line molecular absorption spectroscopy. Diode laser is used for emitting a near-infrared light beam through the sample gas and the light is detected by a receiver. Laser diode output is tuned for a gas specific absorption line. Cross-sensitivities of the method is insignificant since the laser light is spectrally much narrower than the gas absorption line (Siemens 2013).

VTT uses Siemens LDS 6 analyzer for NH<sub>3</sub> measurements. Transmitter and receiver units are installed to a mobile test set-up (Figure 14), so that the laser can be used in various test cells and it can be used also for field measurements. An external pump is used for generating sufficient exhaust flow through the laser or the laser can be part of the exhaust line. The effective laser path length is ca. 60 cm. Test set-up includes possibility to heat the exhaust tube around the laser path.

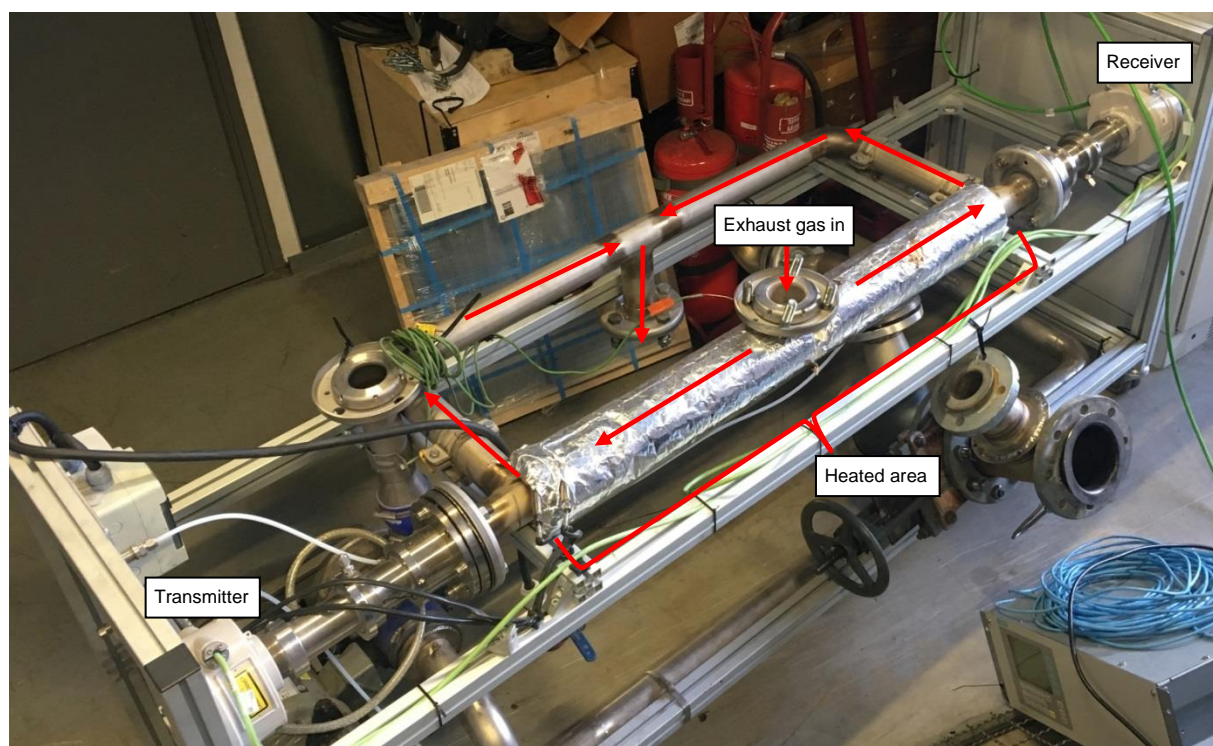


Figure 14. LDS analyzer test set-up. Arrows indicate the flow path of sample gas.

#### 4.3.1.3 Delphi NH<sub>3</sub> sensor

Delphi NH<sub>3</sub> sensor was introduced at 2010 in SAE World Congress. The sensor is designed for the OBD of diesel engines for NO<sub>x</sub> reduction control (Chabot 2010). The specifications were given at the 2007 Diesel Engine-Efficiency & Emissions Research Conference (D. Wang 2007). Delphi

sensor is based on electro-chemical cell where solid oxide electrolyte ionizes oxygen and carries oxygen ions to the other side of the oxide layer where the ions reduce  $\text{NH}_3$  to  $\text{N}_2$  and  $\text{H}_2\text{O}$ , and in this reaction EMF is formed as a signal proportional to  $\text{NH}_3$  concentration. A report on the use of Delphi  $\text{NH}_3$  sensor for SCR control, interferences with other gases and response to varying measurement conditions has been published by SAE International (Wang 2008). According to Wang et. al.  $\text{SO}_2$  has strong cross interference to sensor but other common exhaust gas compounds after SCR do not have significant cross interferences.

There are several manufacturers of  $\text{NH}_3$  sensors and analyzers for process and personnel protection applications (see e.g. Sensidyne  $\text{NH}_3$  gas detectors (Sensidyne 2018), ABB diodelaser for  $\text{NH}_3$  slip measurement (ABB 2018) ). In addition to Delphi only Swedish Sensic offers an  $\text{NH}_3$  sensor for heaters, boilers and CHP plants as well as for diesel engine exhaust after-treatment systems (Sensic 2018).

### **4.3.2 Measurements campaigns**

#### **4.3.2.1 Laboratory measurements at VTT**

Comparison of different  $\text{NH}_3$  measurement technologies was performed at VTT's Engine and vehicle laboratory with diesel bus. Measurements were performed with bus on a heavy-duty chassis dynamometer since the  $\text{NH}_3$  sensor is designed for automotive applications. Bus was equipped with SCR and DPF and it was driven on a heavy-duty chassis dynamometer. A sulphur free ( $\text{S} < 10$  ppm) fuel was used for the measurements. Following devices were used for  $\text{NH}_3$  measurements:

- MKS 2030 FTIR
- Siemens LDS 6 Laser Gas Analyzer
- Delphi  $\text{NH}_3$  sensor (unused sensor)

FTIR uses extractive sampling, which consist of heated sampling lines, filter and pump. Lines, filter and pump were heated up to  $190^\circ\text{C}$ .  $\text{NH}_3$  sensor was installed on the exhaust pipe close to FTIR's sampling location. The LDS was in the exhaust line after the sensor and FTIR. Only part of the exhaust gas was guided to LDS and rest was by-passed the instrument. Otherwise the LDS measurement pipe would have created too much back-pressure for the vehicle. For creating enough flow through laser set-up, an adjustment valve was added to the exhaust line. Schematic of the measurement arrangement is presented in Figure 15.

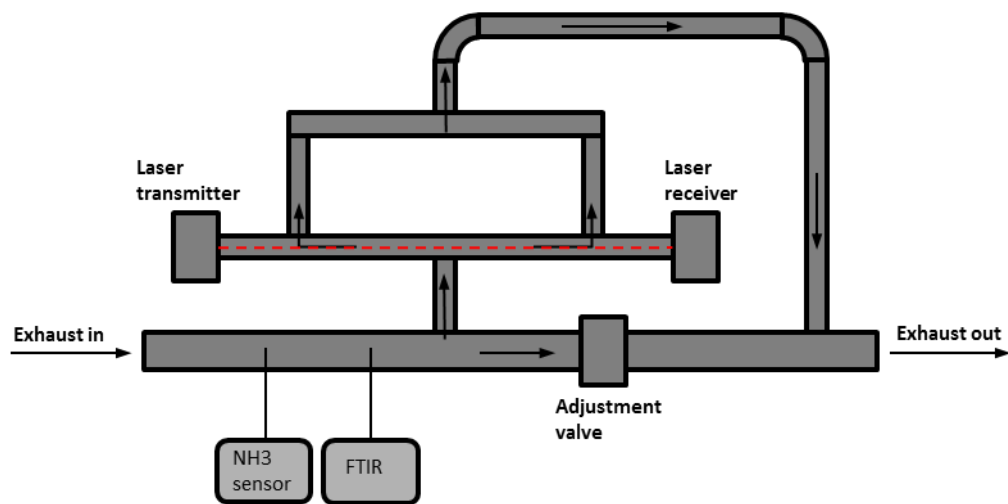


Figure 15. Measurement set-up for truck measurements.

Measurements were performed on Braunschweig test cycle and World Harmonized Vehicle Cycle (WHVC), which are widely used test cycles for heavy-duty vehicle emission measurements. In the cycles the vehicle speed and engine load varies on second-by-second basis simulating real driving conditions. In addition to transient cycles, measurements were performed on constant 85 km/h speed.  $\text{NH}_3$  concentration after the SCR catalyst was varied using different urea dosing levels. On constant speed the  $\text{NH}_3$  concentrations were varied from a few ppms up to ca. 25 ppms. On transient test cycles the  $\text{NH}_3$  peaked up to 10-20 ppms.

#### 4.3.2.2 $\text{NH}_3$ ship trial 1

Ship trial 1 was part of the measurement campaign organized by SEA-EFFECTS BC project on a modern cruiser ship (see Chapter 4.2.3.3). Purpose of the  $\text{NH}_3$  measurements was to test the  $\text{NH}_3$  sensor's response to altering  $\text{NH}_3$  concentrations with HFO and MGO fuels and compare the results with FTIR measurement technology. The sensor was installed to the exhaust line after the SCR system using installation probe (Figure 16). With the installation probe the sensor was inserted in the exhaust line to ca. 0.5 m depth. Pressurized air was used for cooling the sensor and wiring inside the probe.



Figure 16. On the left the sensor installation probe, in the middle sensor tip at the end of the probe, on the right sensor installed in the exhaust line.



FTIR analyzer used in the measurements was Gasetm DX4000. Sampling line for the FTIR consisted of heated pre-filter and heated sampling lines. The temperature for heated lines and filter were set to 180 °C.

Measurements were performed using three different urea injection levels; “Low urea feed”, “Normal urea feed” and “High urea feed”. With the “Low urea feed” the aim was to ensure that there is no NH<sub>3</sub> after the SCR for defining the sensor “zero” level and the “High urea feed” was used for increasing the NH<sub>3</sub> concentration after the SCR. “Normal urea feed” was the normal operation of the system. Measurements were repeated with HFO and MGO.

#### 4.3.2.3 NH<sub>3</sub> ship trial 2

Trial 2 was a long-term test for the sensor in HFO application and lasted nearly four months. It was carried out on a modern cruiser ship. Same installation probe was used for the sensor installation as in trial 1. The needed accessory (computer, power supply, etc.) was placed close to sensor in secured box (Figure 17). The computer was enable to connect to 3G/4G network when network was available in ports and that way it was possible to monitor the system from VTT’s facilities and transfer data.



*Figure 17. NH<sub>3</sub> sensor installation on ship trial 2. Sensor installed in the exhaust line on left hand side and accessory box for computer, power supply etc. on right hand side.*

The sensor was installed in the exhaust line to a location where exhaust gas from two engines are compiled. The other engine had a SCR system and the other did not have any aftertreatment devices. Typical exhaust gas temperature at the installation location is 200 - 250 °C. This installation location ensured that the sensor was exposed to the exhaust gas as much as possible during the four months trial. The sensor data during the trial was recorded with a laptop computer left in the ship and data from the ship’s recording systems was available for supporting the sensor data analysis (e.g. SO<sub>2</sub>, engine loads, urea feed, etc.). The trial was performed with an unused sensor

and it was tested at laboratory before and after trial to find out the trial's effect on the sensor performance.

#### 4.3.2.4 NH<sub>3</sub> ship trial 3

The purpose of the Trial 3 was to test unused Delphi NH<sub>3</sub> sensor on a ship using low sulphur residual fuel (S<0.1%). Length of the trial was 37 days. For the trial 3 a new installation probe was designed and manufactured at VTT. The sensor was installed in the exhaust line using a side flow installation probe (Figure 18). Probe has inlet orifice towards flow and outlet orifice to opposite direction. Flow through the probe is generated by the pressure difference over the orifices. Probe is attached to exhaust line using DN80 flange. It has connections for NH<sub>3</sub> and NO<sub>x</sub> sensors, thermocouples measuring exhaust gas temperature from the main and side exhaust flows and two connections for e.g. FTIR measurements (side flow and main exhaust flow, Figure 189 and Figure 1920).

Using the new installation method there was no need for the pressurized air. Also this installation probe could be easily equipped with sheet air if part time operation of the sensor is needed. The temperature from the side flow was measured during the trial for ensuring that there is a flow and sufficient temperature conditions for the sensor. At the beginning of the trial also a FTIR measurement (Gasetmet DX4000) was performed on ship to get some background information about the exhaust gas emissions. Figure 20 presents the installation on ship.



Figure 18. NH<sub>3</sub> sensor installation probe used in ship trial 3.

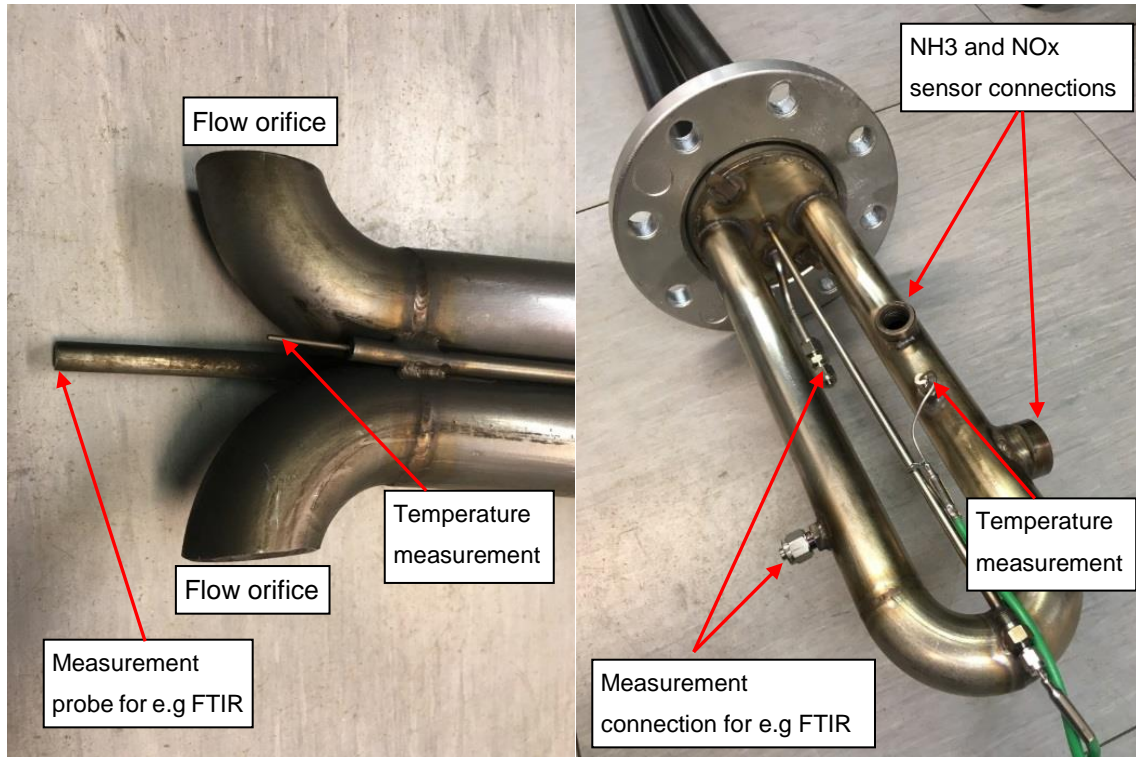


Figure 19. Details of the sensor installation probe used in trial 3.

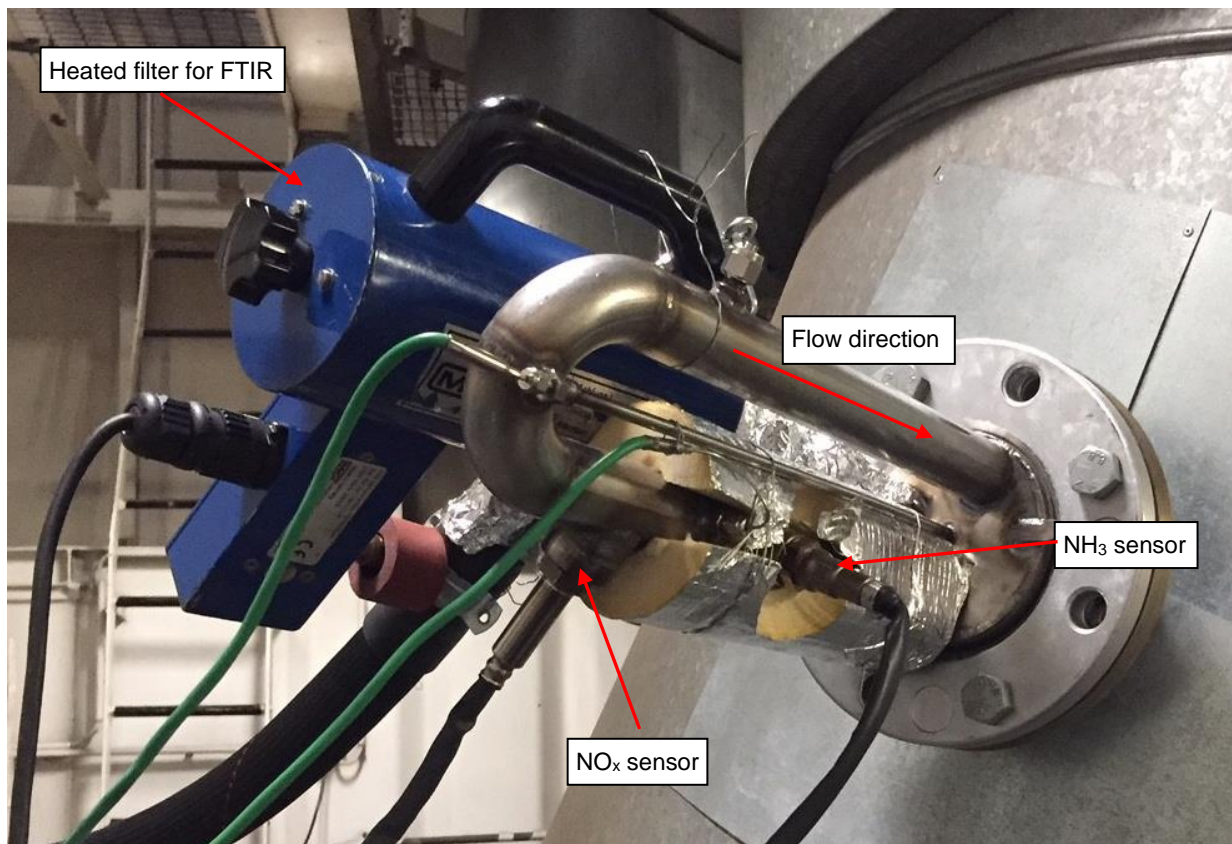


Figure 20. Sensor probe installation in trial 3.

#### 4.4 Methane catalyst study

Gas engines with lean-burn technology are known to have rather low emissions. However, some unburned fuel i.e. natural gas (mainly composed of methane) can end up in the engine exhaust gas. One way to decrease the methane emissions is the utilization of an oxidation catalyst. However, the  $\text{SO}_2$  and water present in the exhaust gas has found to inhibit the oxidation of methane and therefore a regeneration procedure needs to be developed in order to maintain the catalyst efficiency. In this work the regeneration of a methane oxidation catalyst (MOC) by  $\text{H}_2$  was studied.

The research facility included a passenger car gasoline engine that was modified to run with natural gas. The selection of driving condition was based on the emission levels. The target was to mimic the emission levels of a relevant power plant engine. The engine with the test facility was presented in detail in (Murtonen 2016). The engine was operated with a lean air-to-fuel mixture. For the present study, only one engine driving mode was utilized. The exhaust gas flow and temperature (measured upstream of the catalysts) were adjusted independently, and therefore, it was possible to keep the exhaust gas composition and flow constant while changing only the temperature.

The natural gas was from Nord Stream and was high in methane content (>95%). The sulphur content of the gas was below 1.5 ppm. The lubricating oil sulphur content was 8000 mg/kg, density was  $889.7\text{kg/m}^3$  and viscosity at  $100\text{ }^\circ\text{C}$  was  $13.96\text{ mm}^2/\text{s}$ .

The methane oxidation catalysts ( $\text{Pd/Pt-Al}_2\text{O}_3$  catalysts) was similar to the MOC studied earlier in combination with selective catalytic reduction (Lehtoranta 2017). The earlier study, however, included no ageing or regeneration experiments. Prior to experiments the catalyst was preconditioned by ageing for 48 h in the selected driving mode with an exhaust gas temperature of  $400\text{ }^\circ\text{C}$  and exhaust flow of  $80\text{ kg/h}$ . The actual experiments were performed at  $500\text{ }^\circ\text{C}$  with an additional experiment at  $550\text{ }^\circ\text{C}$ . The catalyst set-up is presented in Figure 21 and the engine out exhaust gas composition at the selected driving mode is presented in Table 2.

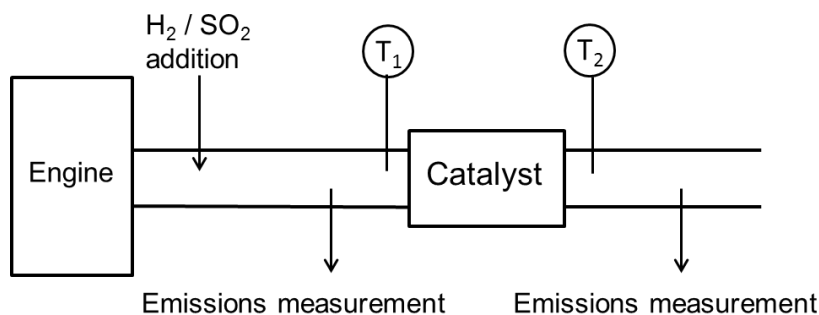


Figure 21. Exhaust gas after treatment installation.

*Table 2 Engine out emissions at the selected driving mode in the beginning of the experiments*

Torque	Speed	Power	NO <sub>x</sub>	CH <sub>4</sub>	CO	CO <sub>2</sub>	O <sub>2</sub>
70 Nm	2700 rpm	20 kW	230 ppm	740 ppm	420 ppm	6.9 %	5.6 %

The experiments included a 190 h at the same driving mode (see Table 3). During the experiments, additional SO<sub>2</sub> was fed into the catalyst in 20 h periods until 80 h was reached following with a longer period of 70 h and again continued with 20 h periods until 190 h was reached. This SO<sub>2</sub> fed (together with the sulphur from the natural gas and lubricating oil) lead to an SO<sub>2</sub> level of 1.5 ppm in the exhaust gas. After each 20 h, H<sub>2</sub> was fed into the catalyst at concentrations of 2-2.5% in order to study how the catalyst regenerates. Specifically, after the first three '20 h ageing' periods 2% of H<sub>2</sub> was fed for 15 min, while the following regenerations were done with 2.5% H<sub>2</sub>. After the 190 h ageing one additional 20 h ageing was done at higher exhaust temperature of 550 °C following by regeneration with 2% H<sub>2</sub>.

*Table 3 Description of the experiment.*

<b>Exhaust temperature</b>	500 °C
<b>20 h ageing periods</b>	SO <sub>2</sub> level in exhaust 1,5 ppm
<b>Regeneration in 20h periods:</b>	H <sub>2</sub> addition:
20h	2 % H <sub>2</sub> for 15 min
40 h	2 % H <sub>2</sub> for 15 min
60 h	2 % H <sub>2</sub> for 15 min
80 h	2.5 % H <sub>2</sub> for 15 min
150 h	2.5 % H <sub>2</sub> for 30 min
170 h	2.5 % H <sub>2</sub> for 30 min
190 h	2.5 % H <sub>2</sub> for 30 min
<b>Total ageing time</b>	190 h
<b>Additional</b>	+ 20 h ageing at 550 °C followed by regeneration with 2% H <sub>2</sub>

In general, emission measurements we done in the beginning of the experiment, after the 20 h ageing, after the regeneration phase, again after the next 20 h ageing and so on. Every time after the regeneration, the emissions were monitored for 4 hours before the next 20 h ageing period.

Emission measurements included a Horiba PG-250 analyser used to measure NO<sub>x</sub>, CO, CO<sub>2</sub>, and O<sub>2</sub>. CO and CO<sub>2</sub> were measured by non-dispersive infrared, NO<sub>x</sub> by chemiluminescence and O<sub>2</sub> by a paramagnetic measurement cell. Exhaust gas was dried with gas-cooler before it was measured by Horiba.

Online SO<sub>2</sub> emissions were determined by a Rowaco 2030 1 Hz FTIR Spectrometer equipped with an Automated MEGA-1 (miniMEGA) sampling system. The detection limit for SO<sub>2</sub> was 2.5 ppm. An agilent 490 MicroGC was used to measure the hydrocarbons and hydrogen. The detection limits for ethane, ethene, and propane were approximately 2 ppm, for methane 10 ppm, and 100 ppm for hydrogen. In addition, multiple gaseous components were measured by two Gaset DX-4000 FTIR spectrometers, one placed upstream and the other downstream of the catalyst.

## 5 Results

### 5.1 PM and PN studies

#### 5.1.1 Verification of movable PM-SDS at VTT's laboratory

As a part of the project VTT build PM-SDS for on-board PM measurements as described in Chapter 4.2.1.3. The main goal was to have a PM measurement system, which is easy to move around on ships, even in tight spaces. The PM-SDS needed to be compared with commercial system for verifying the correct operation of the new device. The comparison was made at VTT's laboratory on heavy-duty chassis dynamometer with diesel truck. VTT's Volvo FL6 Euro II emission level truck was used for the measurements for getting sufficient particle concentrations. The particle concentration was varied between 11-17 mg/Sm<sup>3</sup> during the measurement period. Measurements were performed with four different DRs (5, 10, 15 and 20) and with each DR four repetitions were measured. DR 10 was measured on two different days.

Figure 22 presents the results of the comparison. The presented results are averages of four repetitions. With DRs 5 and 15 the difference between Smart Sampler and PM-SDS is below 1.5%. With DR 10 the PM-SDS results are 18% higher compared to Smart Sampler. The measurements with DR 10 were repeated on two days and the flow calibration of devices was checked on both days. The difference between Smart Sampler and PM-SDS was the same on both days. The reason for the high difference was not found during the measurement campaign. Only 2 % error on total sample flow or on dilution air calibration could have caused the 18% difference between the instruments. With DR 20 the difference between Smart Sampler and SDS increases significantly and the result measured with SDS seems to be too high. For mass flow controlled partial dilution systems high DRs are challenging and it might be so that the performance of mass flow controllers of PM-SDS is not good enough for DRs above 15.

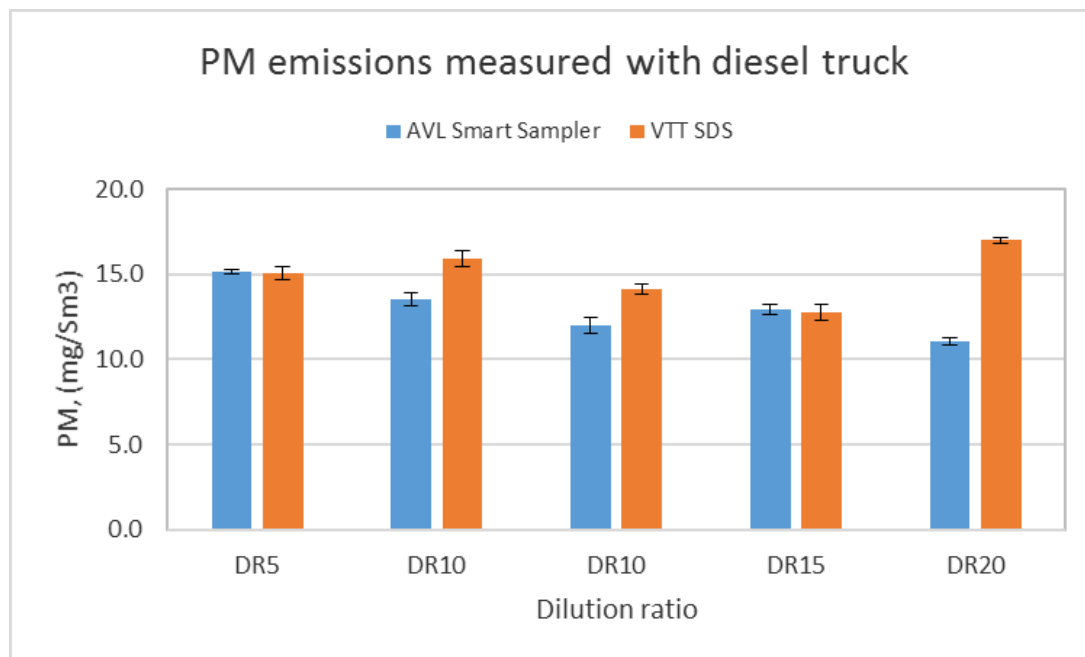


Figure 22. PM results measured with diesel truck on VTT's heavy-duty chassis dynamometer.

With Smart Sampler the PM result seems to decrease when DR is increased. This is a known effect of DRs with partial flow dilution system and especially with high sulphur fuels. With low sulphur fuels the phenomena is not that strong but still exists. Increasing the DR lowers the PM result by decreasing the volatile portion of the PM (Ntziachristos, et al. 2016), (Ntziachristos, Saukko and Rönkkö, et al. 2016), (Ristimäki, Hellen and Lappi 2010).

Results of the comparison are extremely good with DRs 5 and 15 but poor on DR 10. The result with DR 20 is unacceptable. More work would be needed for finding out the reason for large difference between instruments at DR 10, which is the most typical DR used in PM measurements.

### 5.1.2 Filter material comparison for PM measurements and role of back-up filters

Figure 23 presents the results of filter material comparison for PM sampling from dual-fuel marine engine in laboratory and from marine engine E3 on-board ship B using the four types of filter materials, two PTFE-types, one PTFE bonded glass fiber and one quartz quality filters.

Detailed information of the filters are presented in Chapter 4.2.1.4. In the dual-fuel engine tests, comparison was made using 25 % engine load and the engine was ran with LFO. With each filter type two repetitions were conducted.

The result in laboratory showed 9% lower results for Pallflex Teflo and Whatman PTFE filters compared to Pallflex TX40 filter. Chase et al. has reported similar results and the according to their studies the artefact is caused by gaseous hydrocarbons absorbed on Pallflex TX40 filter (Chase, et al. 2004). For engine E3, four different filter materials gave comparable PM results, particularly at

PM concentrations below  $100 \text{ mg/m}^3$  (Figure 23). At higher PM concentrations, PTFE Whatman collected lower amount of aerosols than other filters. Noticeable is that larger difference in collection efficiency of filters tested was observed between two types of PTFE filters (Whatman and Pallflex) than between PTFE and PTFE bonded glass fiber filter (Pallflex TX40). Quarz filters collected more condensable semivolatile material at high PM concentrations than other filters. Pallflex TX40 and PTFE Whatman filters collected similarly sulphates. Quarz filter collected the highest amount of aerosol and resulted in the largest spread in the results.

As a conclusion, PTFE bonded glass fiber filters, and particularly quarz filters, tend to collect more material than the PTFE filters. However, at low PM concentrations this difference was not always consistent.

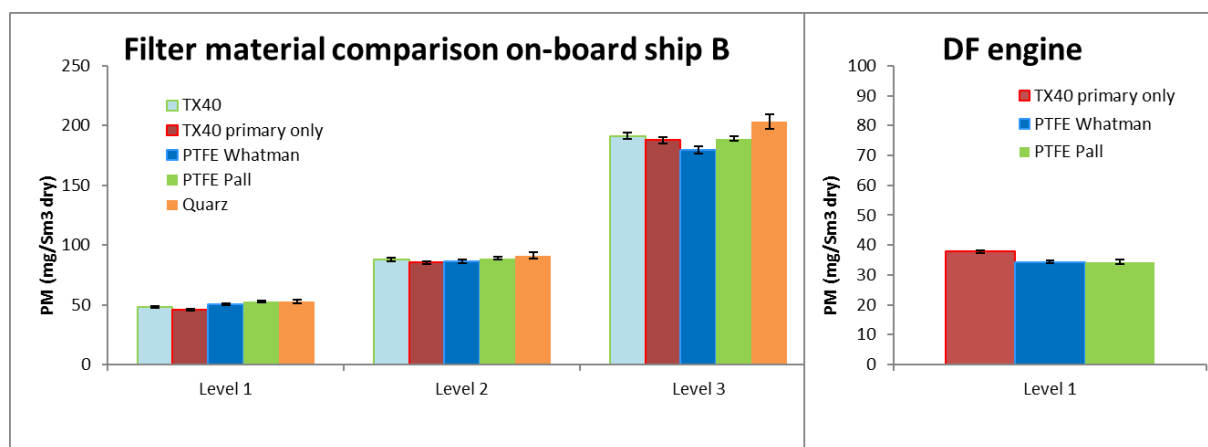


Figure 23. Comparison of filter materials for collecting PM from marine engine (E3) exhaust.

On the on-board measurements, back-up filters were used in the PM measurements. Due to analytical purposes the loaded PM filters were stored in a portable refrigerator before bringing filters back to laboratory. For E2 engine, close to 300 filters were used for PM collections, including the back-up and reference filters. PM mass on the back-up filters was in most cases below 5% of the total PM mass (Figure 24). Only for samples after SCR, higher share of PM mass on the back-up filters compared with the total PM was observed. This material was not analysed. For E3, mass observed in the back-up filters was in most cases below 4% of PM, and material on back-up filters did not contain sulphates. Slight amount of material found in back-up filters is assumedly organic matter in most cases, however, not necessarily for SCR.

Back-up filters are not typically used in the measurements of large engines. In some cases, where more information is desired on the characteristics of new technologies, or for other research purposes, back-up filters can be useful.



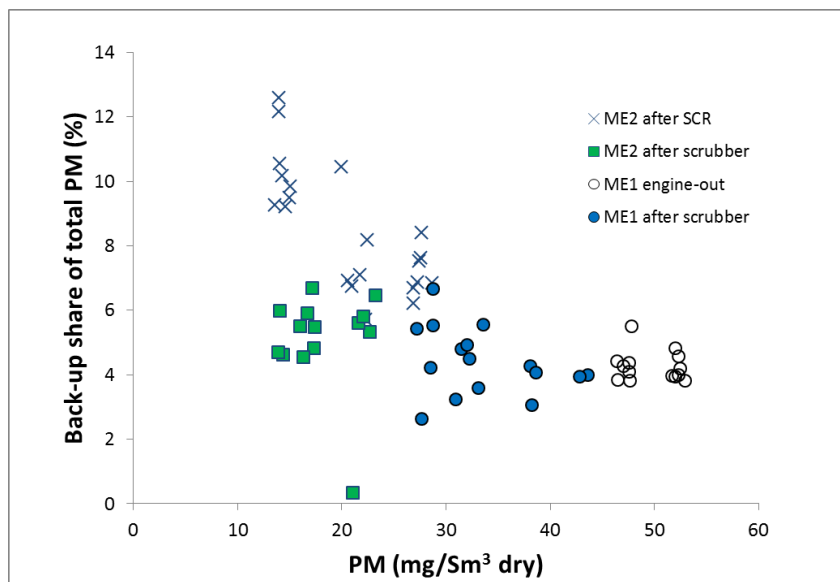


Figure 24. Share of PM mass on the back-up filter of total PM mass.

### 5.1.3 Comparison of Pegasor PPS-M sensor and VTT's PN measurement system

Figure 25 and Figure 26 presents the particle number results measured with the approved PN-system (labeled as CPC in figures) and Pegasor PPS-M sensor with DF engine. In DF-mode the results with Pegasor sensor were 1.7-1.9 times higher compared to PN-method on 75, 50 and 25% loads. For 100% load there is no result from Pegasor sensor. On 10% loads the Pegasor sensor showed 16 and 53 times higher values compared to PN method depending on which engine parameter set the 10% load was ran. It is possible that on 10% load the number of volatile particles is very high and this can partly explain the remarkable increased difference between Pegasor sensor and CPC. In diesel measurements the results with Pegasor sensor were 1.2-1.6 times higher in comparison with PN-system.

The comparison between PN-method and Pegasor sensor is a bit difficult. PN-method is designed for measuring solid particles. The sampling method removes volatile particles very efficiently. The Pegasor sensor dilutes and measures the particles at high temperature (sample lines/ dilution 180 °C, sensor 200 °C). It is assumed that in those temperatures the share of volatile particles is typically relatively low. However, it is likely that there are some volatile particles present in the sample gas. Secondly, the cut-off curve for 23 nm particles is much steeper for CPC used in PN-method than for Pegasor sensor. This means that the Pegasor sensor measures significant amount of particles below 23 nm and when running on natural gas a significant number particles are in smaller size classes than 23 nm (Lehtoranta, et al. 2017), (Alanen, et al. 2015), (Anderson, Salo and Fridell 2015). Thirdly, the Pegasor sensor has been calibrated assuming that the mean particle size is 50 nm. If the mean particle size is bigger the sensor's sensitivity is higher resulting a higher output from the sensor. In case of diesel exhaust it is likely that the particle number is above 50 nm. According

to sensor manufacturer most of the sensor's users calibrate the sensor against CPC for different applications. This would be also needed in this case to get more accurate results.

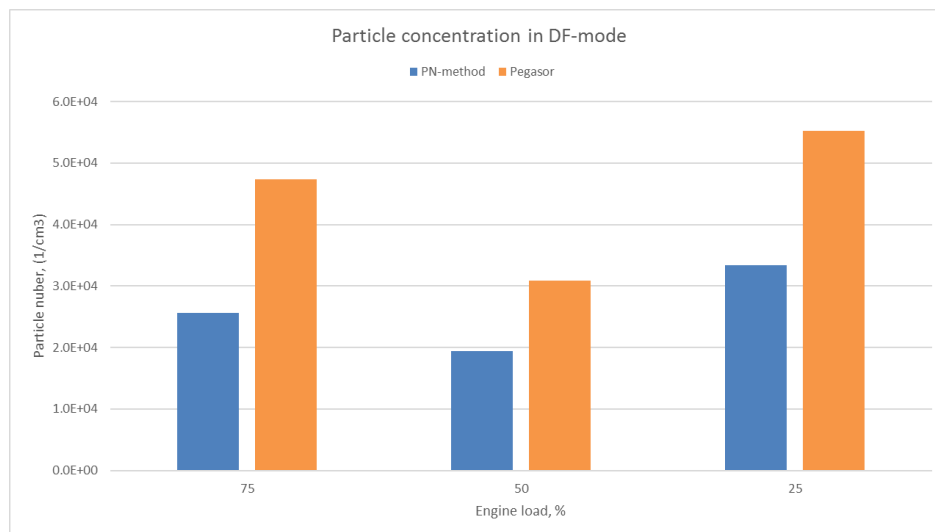


Figure 25. PN results with Pegasor sensor and VTT's PN method, engine in DF-mode.

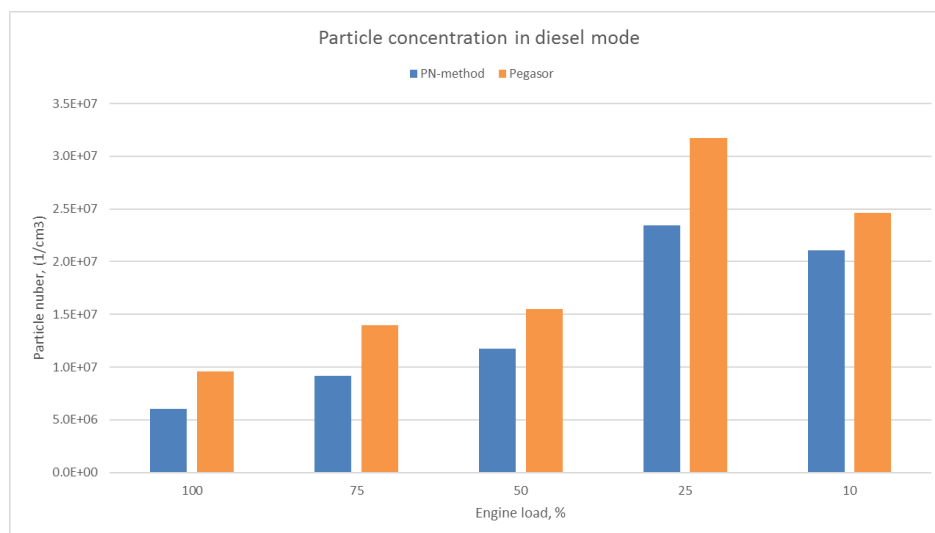


Figure 26. PN results with Pegasor sensor and VTT's PN method, engine in diesel mode.

#### 5.1.4 PM and PN results from DF engine and in onboard ship campaigns

Figure 27 presents the PM and PN emissions from the DF engine and from three marine engines E1, E2 and E3 during on-board ship measurement campaigns. The on-board measurements campaigns organized by SEA-EFFECT BS and EnviSum projects are described in Chapter 4.2.3. Engines operated with HFO and one of the engines was also measured with MGO.

For DF engine using diesel fuel, the PM emission were in range from 63 to 291 mg/kWh. PM emission was the lowest on 100% load and highest on 10% load. In DF mode, the PM emissions were 77-91% lower compared to measurements with diesel. The PN emissions followed the same trend with PM and ranged from  $3.25 \times 10^{13}$  to  $2.82 \times 10^{14}$  with diesel fuel. With natural gas the PN

emissions were over 99% lower compared to diesel. The lowest particle number emission was on 75% ( $1.26 \times 10^{11}$ ) and the highest on 10% load ( $2.39 \times 10^{12}$ ).

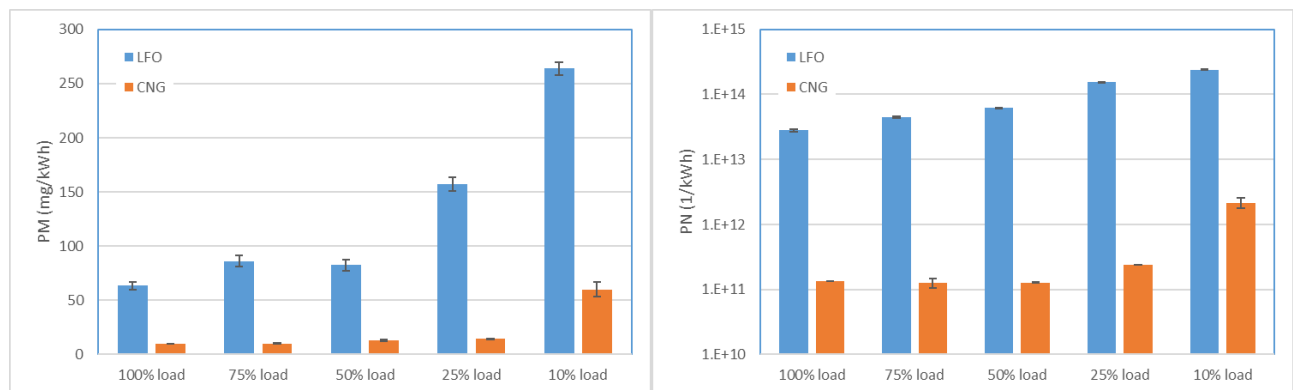


Figure 27. PM and PN results measured with DF marine engine.

Figure 28 presents the results from both ship campaigns (E1, E2 and E3). The PM emissions after the scrubber were below 156 mg/kWh for E1, below 237 mg/kWh for E2 at 40% and 75% loads and 239 mg/kWh for E3 at 63-66% load (1.4 g/kg fuel, 0.24 g/kWh) using HFO. PM reduction over the scrubber was 17-45% for E1 and E3. Engine-out PM concentrations were higher when using HFO than MGO mainly due to the differences in the fuel sulphur induced sulphates in PM. For the MGO fuel, PM was low already at engine-out exhaust.

The PN emission of E1 and E2 (modern engines) was independent of load and there was no changes in particle numbers before and after scrubber. Size distributions revealed that number of particles was high in size range 20 to 30 nm before scrubber (Timonen , et al. 2017). After the scrubber this particle mode is vanished.

Based on the size distribution curves and PN results before and after the scrubber it seems that the number of volatile particles in the exhaust gas is high before the scrubber. Those particles are not detected by the PN method used by VTT. Therefore the PM reduction was clear over the scrubber but there was no change the PN emissions measured according to the ISO8178-1:2017.

E2 was measured also with MGO before the scrubber on 40% engine load. With MGO the PN emission before the scrubber was 89% lower compared to PN emission with HFO measured after the scrubber. After scrubber, PN emissions with E3 where ca. 3 times higher compared to E1 and E2.

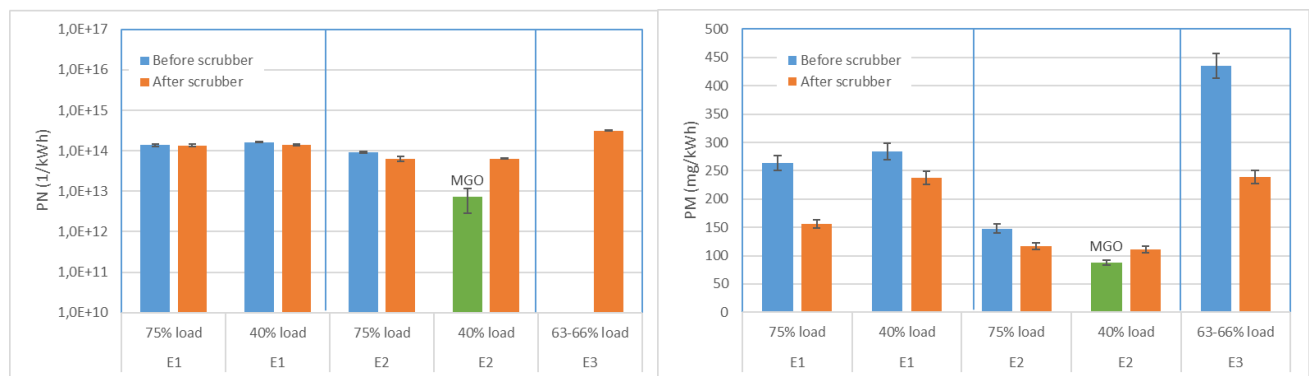


Figure 28. PN (left-hand side) and PM (right-hand side)s measured with ship diesel engines E1, E2 and E3 before and after scrubber.

## 5.2 NH<sub>3</sub> sensor studies

### 5.2.1 NH<sub>3</sub> measurements at VTT's laboratory

NH<sub>3</sub> measurements at VTT's laboratory were performed on heavy-duty chassis dynamometer with Euro VI emission level diesel bus using diesel fuel with below 10 ppm sulphur content. Measurements were performed on constant speed varying urea injection and with two transient cycles (Braunschweig and WHVC). Devices used in the measurements were MKS 2030 FTIR, Siemens LDS 6 laser and Delphi NH<sub>3</sub> sensor.

Figure 29 presents the results from the constant speed measurements. During the first measurement interval (0-1200 s), the laser temperature was still increasing and therefore the signal is going up and down, and fluctuation was seen also in the second interval, while NH<sub>3</sub> concentration measured using sensor was relatively constant. On the third and fourth measurement intervals there was only minor fluctuation in laser signal. As Figure 29 shows, the FTIR gave the lowest NH<sub>3</sub> concentration on most of the measurement intervals. This is the downside of the extractive sampling method when measuring NH<sub>3</sub>, which tends to adsorb on sampling lines and filters. The results obtained with FTIR were not substantially different from those obtained with laser on the second and fourth measurement intervals. The laser and sensor measured equal concentrations on the other measurement intervals, except during the fourth measurement interval. On the fourth interval, the laser gave lower NH<sub>3</sub> result compared to sensor, but equal to that obtained with FTIR.

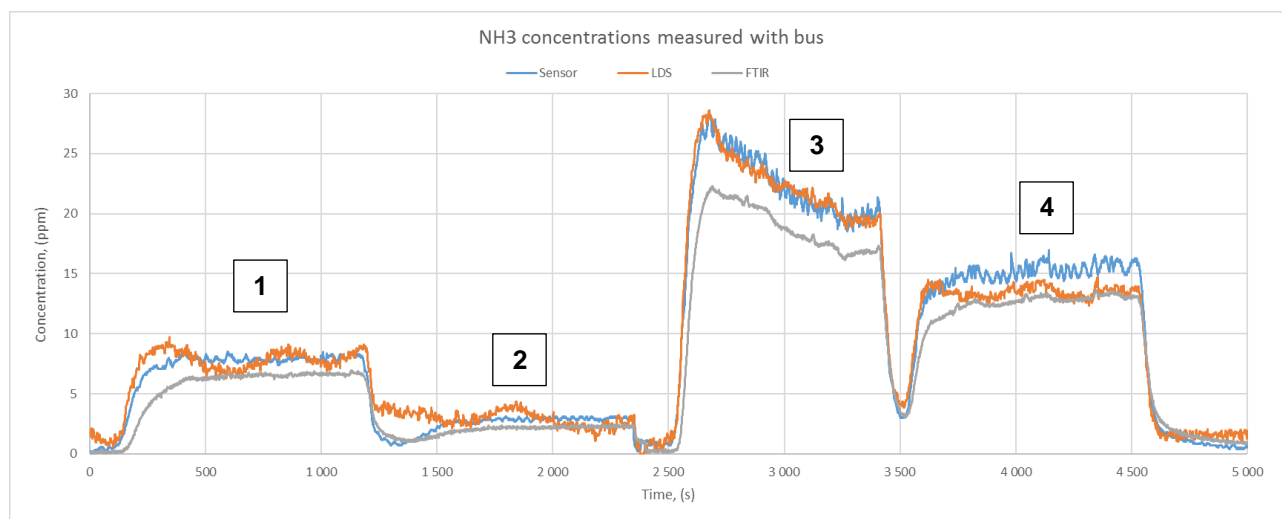


Figure 29.  $\text{NH}_3$  measured on constant speed on chassis dynamometer with varying urea feed.

The Figure 30 presents the averaged concentrations calculated from the data presented in Figure 29. FTIR and sensor both have a strong linear correlation when compared to laser. FTIR would need ca. +17% correction to match the LDS concentration while for sensor the needed correction is less than 1%. However, we note that higher differences than 1% were observed also between sensor and laser in many cases.

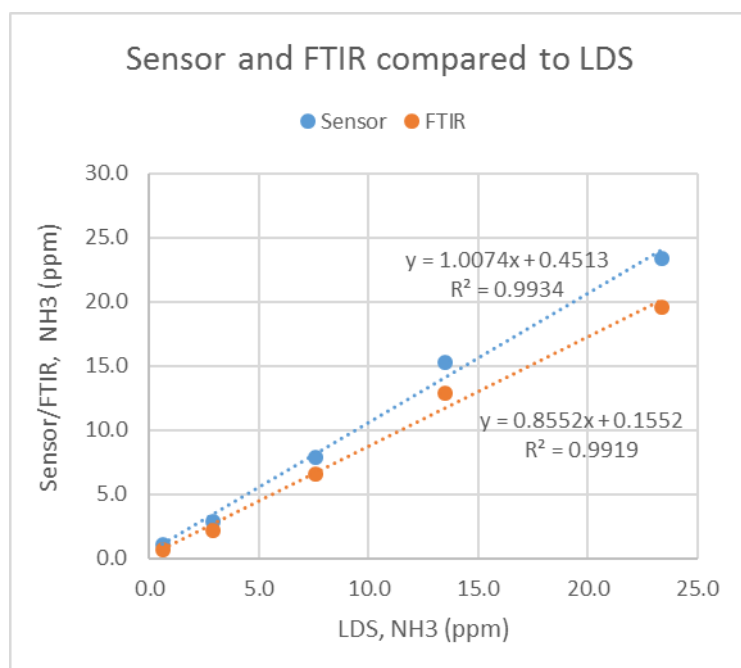
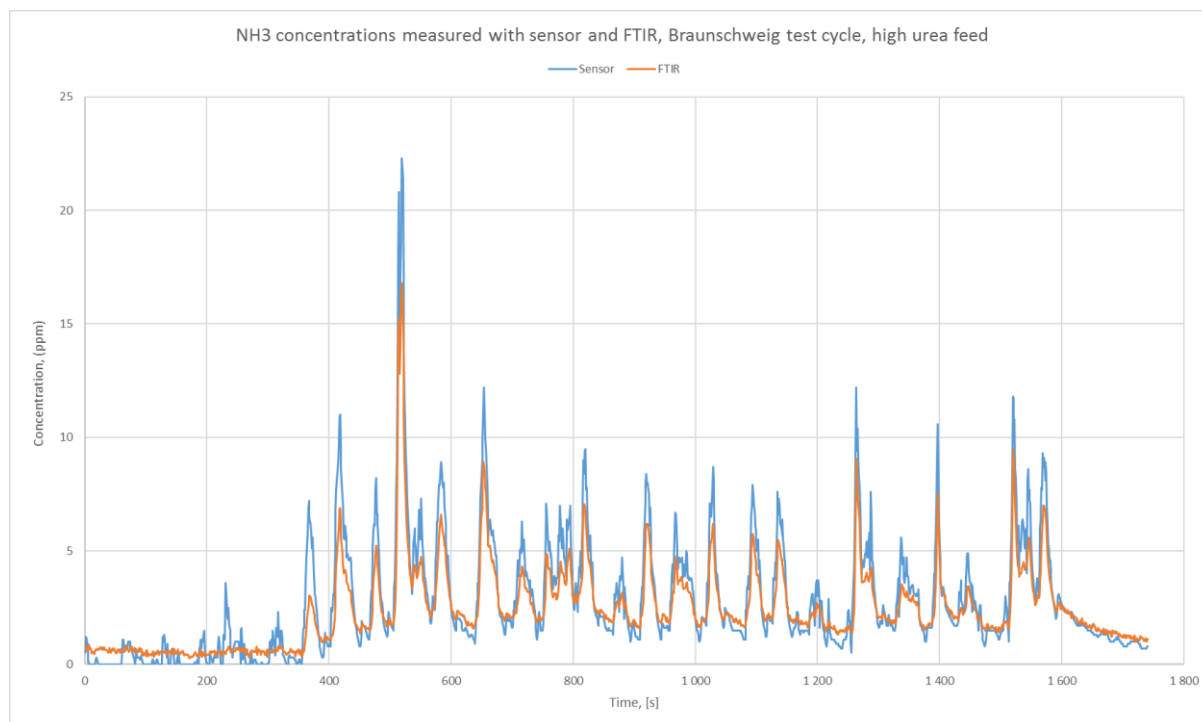


Figure 30. Sensor and FTIR compared to LDS.

On Braunschweig test cycle, measurements were performed only with FTIR and sensor. For this cycle, the urea injection rate was increased for getting  $\text{NH}_3$  slip after the SCR. Figure 31 presents the  $\text{NH}_3$  concentrations measured over the cycle. Both measurement techniques showed fast

response to changing concentrations. The peaks measured by the sensor were somewhat higher compared to FTIR. The overall performance for both devices can be considered good.



*Figure 31. NH<sub>3</sub> concentrations measured with sensor and FTIR from diesel bus exhaust over Braunschweig test cycle.*

NH<sub>3</sub> measurements over the transient WHVC test cycle were conducted using normal urea feed setting, and an increased NH<sub>3</sub> concentration was detected only at the end of the cycle. In Figure 32, two repeated cycles are presented, the length of a one cycle is 1800 s. Basically the NH<sub>3</sub> concentrations were below detection limit for each device until the end of the cycles. Figure 33 presents the NH<sub>3</sub> concentration measured during the last 300 seconds of the cycle. It is noticeable that the LDS showed the highest peaks and FTIR the lowest. The difference between the NH<sub>3</sub> results obtained with sensor and FTIR was higher for the WHVC cycle than for the Braunschweig test cycle. This might be due to different sampling history before the measurements. Before Braunschweig test cycle, some elevated NH<sub>3</sub> concentrations were measured with FTIR and the sampling line and filter was "contaminated" with NH<sub>3</sub>. Before WHVC cycle, relatively long measurement period was conducted without any NH<sub>3</sub> present in the exhaust (zero NH<sub>3</sub> concentrations). We assume that the sampling line was kind of "cleaned" from NH<sub>3</sub> with the sample gas without any NH<sub>3</sub>. However, these phenomena deserve thorough investigation before making solid conclusions.

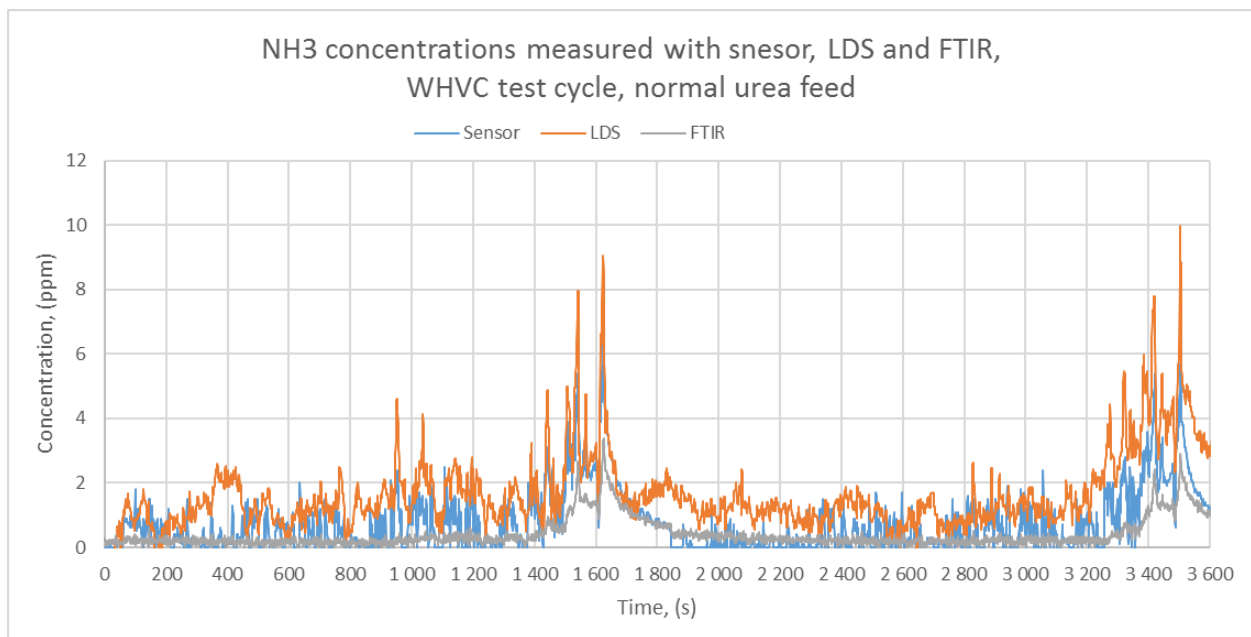


Figure 32. The  $\text{NH}_3$  concentrations measured over the WHVC test cycle with sensor, LDS and FTIR.

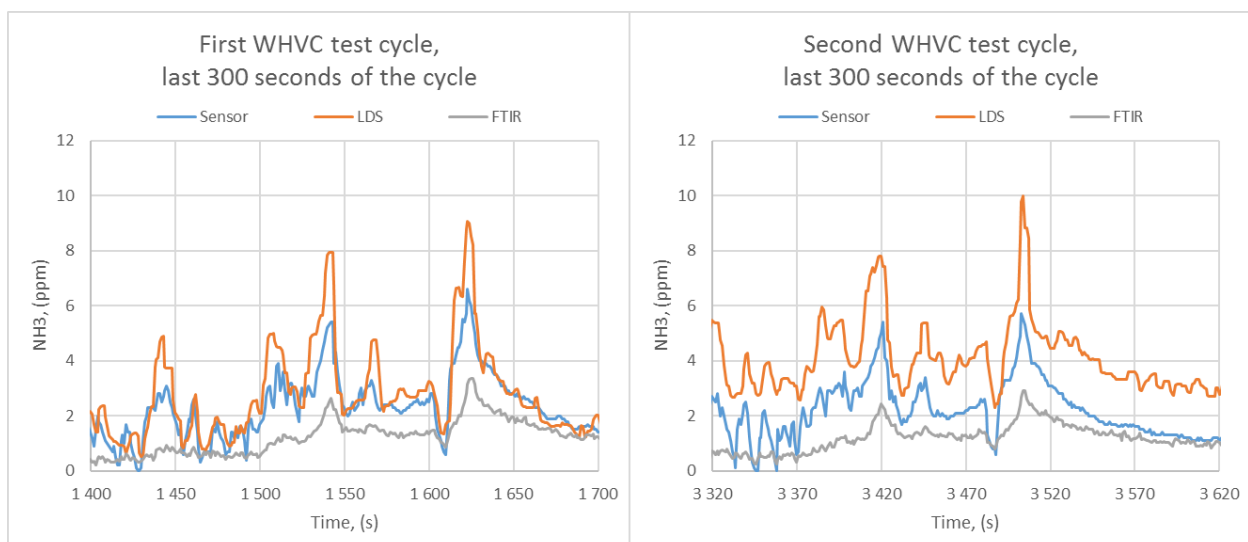


Figure 33. The  $\text{NH}_3$  concentrations measured during the last 300 seconds of the WHVC test cycle.

### 5.2.2 $\text{NH}_3$ ship trial 1

Ship trial 1 included measurements with Delphi  $\text{NH}_3$  sensor and FTIR (Gaset DX4000). Measurements were carried out with two fuels (HFO and MGO) and three different urea injection levels (low, normal and high). The purpose of the trial was to test the  $\text{NH}_3$  sensor with very “dirty” exhaust gas. The sensor is designed for automotive applications with clean exhaust gas compared to ships.

The  $\text{NH}_3$  results from marine engine exhaust using HFO as fuel are presented in Figure 34 (left-hand side). Three different urea feed levels were used: low, normal and high. As can be seen from

the Figure 34, there is no difference on  $\text{NH}_3$  concentrations between low and normal urea feed levels. The sensor showed ca. 15-20 ppm background concentration while FTIR readings were below detection limit. After increasing the urea feed from normal to high, the  $\text{NH}_3$  sensor results slowly increased. The SCR catalyst is known to have storage capacity for excess  $\text{NH}_3$ , and with increased urea injection it takes time before  $\text{NH}_3$  slip appears after the catalyst (Lehtoranta, Vesala, et al. 2015), (Amanatidis, et al. 2014). The  $\text{NH}_3$  concentrations measured with sensor steadily increased to a ca. 55-60 ppm level and leveled off. Instead, the  $\text{NH}_3$  concentrations measured with FTIR started to increase much later, more than one hour later than those measured with sensor. This is due to ammonium sulfate deposit in the FTIR sampling system, which is reported e.g. by Lehtoranta et al. (Lehtoranta, Vesala, et al. 2015). The  $\text{NH}_3$  concentration measured with FTIR continued to increase until the urea feed was switched back to normal level.  $\text{NH}_3$  concentration measured with FTIR peaked at 25 ppm before it started to decrease. The measurement clearly evidenced the how challenging  $\text{NH}_3$  measurement is from exhaust gas in the presence of  $\text{SO}_2$ . The sulfur content of the HFO used in these measurements was 0.65% (m/m) and the  $\text{SO}_2$  concentration of the exhaust gas was some 190 ppm.

When the urea feed was decreased to normal level, the  $\text{NH}_3$  concentration measured with sensor started to decrease after 5 minutes. With FTIR the “memory” of the sampling lines caused a slow increase of the concentration after the change in urea feed level before the concentration slowly decreases.

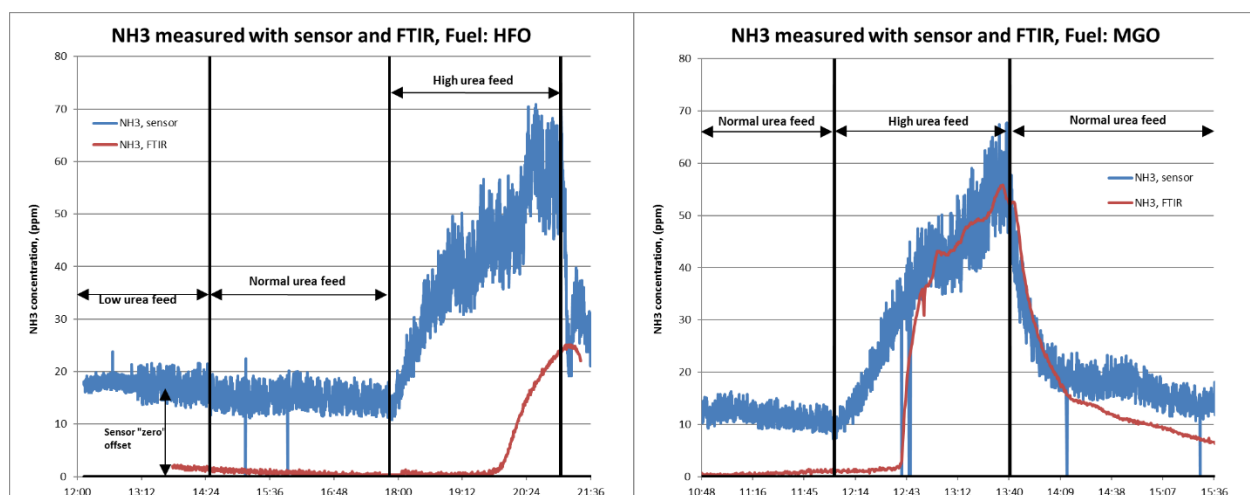


Figure 34.  $\text{NH}_3$  measured with FTIR and  $\text{NH}_3$  sensor. On the left side results with HFO and on the right side with MGO. For Both fuel the urea injection rates were the same.

The right hand side of the Figure 34 presents the  $\text{NH}_3$  results with MGO. The sulfur content of the MGO was 0.078% (m/m) and the  $\text{SO}_2$  concentration of the exhaust gas was just below 20 ppm. With MGO, the  $\text{NH}_3$  concentration measured with sensor began to increase almost immediately after increase of the urea feed. The  $\text{NH}_3$  concentrations measured with sensor reached approximately the same concentration as that measured for HFO before the urea feed decreased back to normal



level. The delay for FTIR in detecting the increase in  $\text{NH}_3$  concentration was shorter when using MGO as fuel than when using HFO, however, delay was still long. The  $\text{NH}_3$  concentration began to increase after 40 minutes from the urea feed increment. However, after the delay, FTIR showed the same  $\text{NH}_3$  concentration as sensor and also followed the same patterns as sensor with a few minutes delay when the  $\text{NH}_3$  concentration decreased.

### 5.2.3 $\text{NH}_3$ ship trial 2

Trial 2 was a long-term test for the sensor on a ship using HFO. Trial lasted nearly four months and sensor was exposed to exhaust gas for 1970 hours (ca. 2.7 months). Trial was performed with unused sensor. Before and after the trial, the performance of the  $\text{NH}_3$  sensor was tested at VTT's laboratory by running natural gas (NG) engine on steady condition and injecting a known amount of gaseous  $\text{NH}_3$  to the exhaust gas. We note that the sensor is not designed for the NG applications. However, according to our experiences the sensor response to  $\text{NH}_3$  with NG engine is linear and repeatable. So even though the sensor's absolute accuracy is not good with NG engine, the engine can be used for checking the possible changes in sensor's performance.

Figure 35 presents three results from the sensor performance tests. The measurement after the trial was performed before any cleanup of the sensor though some of the soot accumulated on the sensor fell down when the sensor was taken out from the installation probe. Before trial the sensor performance was typical for measurements with NG engine (lower than those measured with FTIR). After the trial sensor had a 12 ppm zero point offset. The "Aft trial" curve presents the results without offset correction and "Aft trial corr." curve is corrected with for the 12 ppm offset. Figure shows that sensor performance has significantly changed during the trial. Response of sensor to  $\text{NH}_3$  is still linear, but not as linear as before the trial. The significant change is that the sensor is more sensitive to  $\text{NH}_3$  after the trial than before and sensor readings are equal with FTIR (Gasmeter DX4000) when the 12 ppm offset is taken into account.

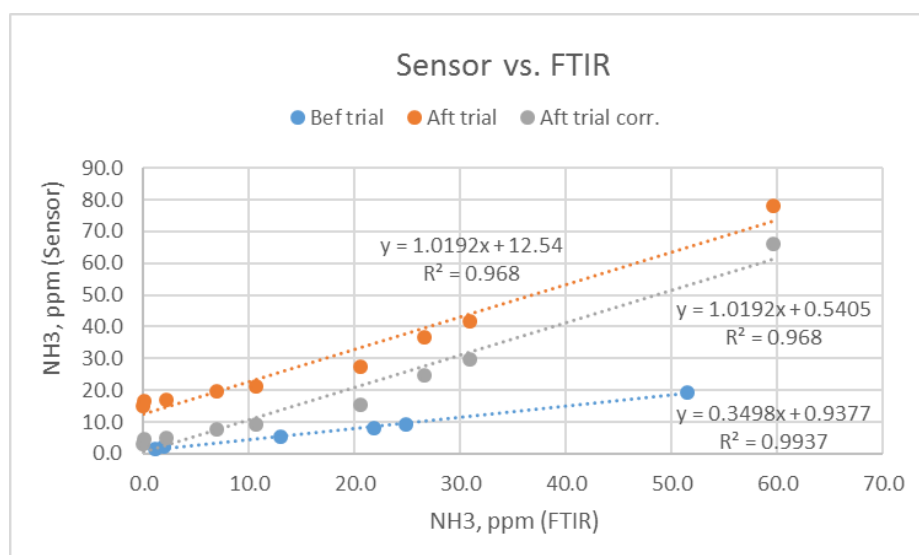
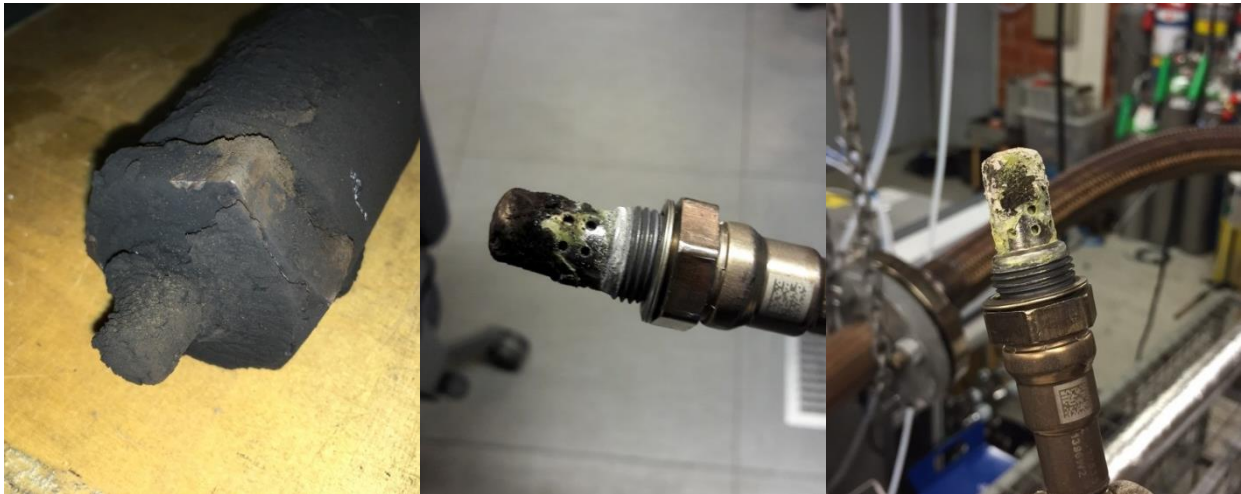


Figure 35.  $\text{NH}_3$  sensor performance tests at laboratory before and after Trial 2.

It is difficult to estimate why the sensor performance has changed during the trial. There was thick particle coating on top of the sensor (Figure 36). The particle coating was partly very porous and it did not seem to block completely the gas flow through the sensor. When sensor was unfastened from the installation probe the particle coating partly felt off (Figure 36). What was left on the sensor was very hard yellowish material, which could not be cleaned by steel brush. It is obvious that if this kind sensor is used on HFO applications, there needs to be cleaning procedure for the sensor. The other possibility is to arrange sheet air for the sensor and the sensor would measure only occasionally. Most likely the high SO<sub>2</sub> concentration and the metals coming from the fuel have affected on sensor performance. HFO can contain e.g. vanadium, nickel and iron. It is known that SO<sub>2</sub> has strong cross interference (D. Wang 2007) to sensor. Particle matter accumulated inside the sensor and having sulfurous compounds may be the source for performance shift.



*Figure 36. Sensor tip after four months trial (left), after taking the sensor off from the installation probe (middle) and after brushing the sensor with steel brush (right).*

In the beginning of the trial, there were problems with the remote access to the computer onboard and sensor data for 1.5 months was lost. However, this was not crucial for the trial, since the main issue was to expose the sensor to the exhaust gas. For the rest of the trial remote access worked and the data sensor was collected.

Similarly to ship trial 1 there was a zero level offset on sensor readings also during ship trial 2. Since the sensor was installed to a location where it was exposed to exhaust gas from engines with and without SCR system, it was possible to define the sensor zero offset when only the engine without SRC was ran. As mentioned earlier, the SO<sub>2</sub> causes cross interference to NH<sub>3</sub> sensor and therefore the sensor showed concentrations for NH<sub>3</sub> even with the engine without SCR. With this sensor, the cross interference shifted sensor's zero level up to ca. 20 ppm with the highest SO<sub>2</sub> concentrations. Figure 37 presents the averaged NH<sub>3</sub> readings calculated from steady engine operation points. It is noticed that the sensor readings are equal from both engines, which indicates that during the trial,



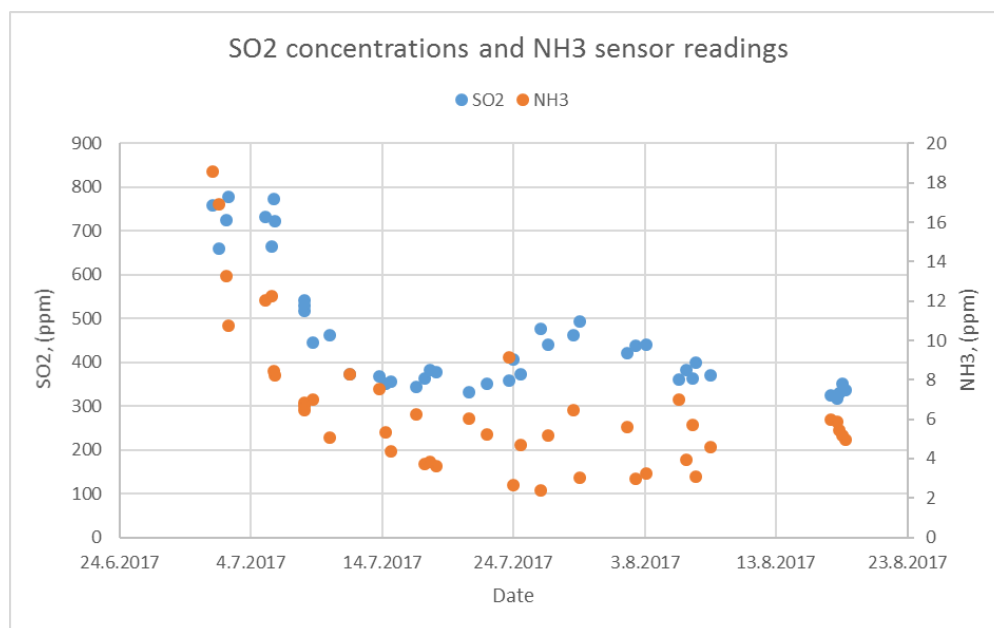


Figure 39. Exhaust gas SO<sub>2</sub> concentration and NH<sub>3</sub> sensor readings during the trial 2.

The ship trial 2 was successful. There was a clear shift in sensor performance, but the sensor did not break down. If the sensor is used only for occasional measurements and if sheet air is used in between measurement periods, the sensor's contamination could be avoided and the sensor could be used for monitoring the SCR system performance. Even though the SO<sub>2</sub> has strong cross interference, sensor can still measure elevated NH<sub>3</sub> concentrations as demonstrated in ship trial 1.

#### 5.2.4 NH<sub>3</sub> ship trial 3

Trial 3 was a long term test on a ship using low sulphur residual fuel (S<0.1%). Trial was performed with an unused sensor. Trial was shorter than trial 2 and lasted 37 days. During that time sensor was exposed to exhaust gas for 332 hours, which is roughly 50% of the ships operation time during the trial. The sensor was very clean after the trial, there was basically no soot accumulated on the sensor (Figure 40). Before and after the trial, the sensor was tested at laboratory and compared to FTIR. Results are presented in Figure 41.



Figure 40. NH<sub>3</sub> sensor after the trial 3, only minor soot contamination on the sensor tip.

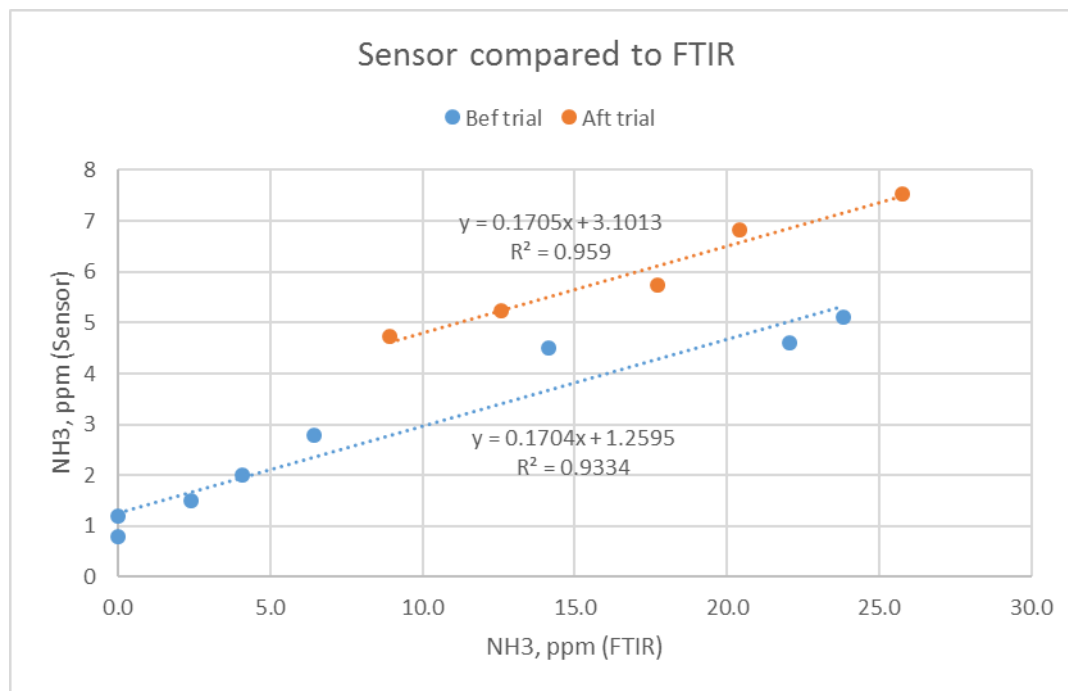


Figure 41. NH<sub>3</sub> sensor performance tests at laboratory before and after trial 3.

Figure 41 shows that the NH<sub>3</sub> concentrations measured with sensor and FTIR showed linear correlation. The slope is the same before and after the trial 3, but there is ca. +2 ppm offset in the result after the trial. We also noted that the sensor did not show any values between 0 and 4.5 ppm in the performance test after the trial. If the concentration went below 4.5 ppm, the sensor reading decreased straight down to zero. This was unexpected, since the sensor worked during the trial and measured concentrations below 4.5 ppm at the end of the trial. The sensor might have been damaged after the trial.

As earlier mentioned (Chapter 4.3.2.4), the different kind of installation probes were used for trial 3 than for trials 1 and 2. The main reason was to exclude the need for pressurized air. One critical issue of the new probe was, that how much the exhaust gas cools down in the probe. On trial 3 the exhaust gas temperature on the main exhaust line and in the sensor installation probe was continuously monitored. The result was that the exhaust gas cools down some 20 to 30 °C in the measurement probe, which is an acceptable result. Measurement location was after the SCR and exhaust gas heat recovery boiler and the exhaust gas temperature at the measurement location was typically ca. 200 °C and the temperature in the measurement probe was ca. 175 °C. The temperature is a bit low for the NH<sub>3</sub> sensor, since the specified minimum temperature is 200 °C. The sensor seemed to work at lower temperature, however, this may affect accuracy of the sensor.

In the beginning of the trial a short FTIR measurement was performed for defining the basic exhaust gas composition. During the measurement, it was noted that there were some very high NH<sub>3</sub> concentrations in the exhaust gas and the condition of the SCR catalyst should be checked and/or the urea injection system should be re-calibrated. Therefore the NH<sub>3</sub> concentrations are reported as

relative values. Figure 42 presents that FTIR and sensor follow the same trend but concentration measured by sensor is much higher compared to FTIR. During the short spikes (ca 0:44 and 0:48) the FTIR reading is ca. 1/3 of the sensor reading. This is most likely due to loss of  $\text{NH}_3$  in the sampling system caused by the formation in ammonium sulphate. During the elevated concentration between 0:57 and 01:03 the FTIR reading is some 50 to 60% of the sensor reading. The same phenomena was seen during the Trial 1 with high sulphur fuel. On those measurements the FTIR reading were some 40 to 45% of the sensor reading. The FTIR response time to increasing concentrations is much faster in trial 3 than trial 1. In trial 3 there were continuous  $\text{NH}_3$  concentrations in the exhaust gas and it is assumed that the FTIR sampling lines and filters saturate with  $\text{NH}_3$  and/or ammonium sulphate over the time which shortens the response time of the sampling system.

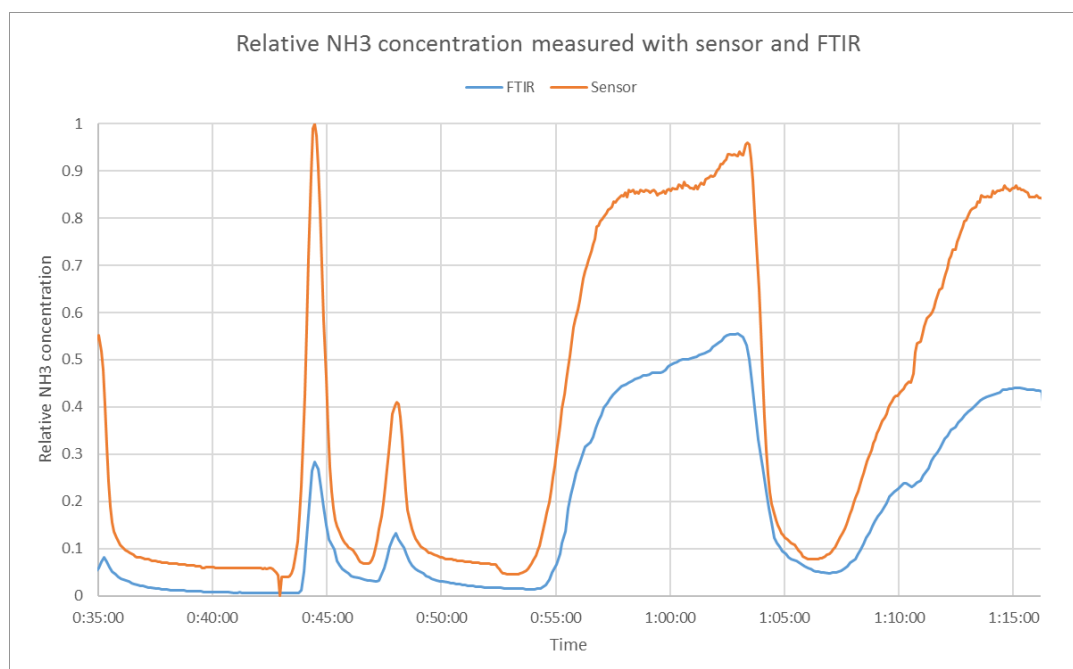


Figure 42. Relative  $\text{NH}_3$  concentration measured with FTIR and  $\text{NH}_3$  sensor.

Figure 43 presents the  $\text{NH}_3$  sensor data and engine load during the trial 3. The engine was not operated 23.12.2017-9.1.2018 due to problems with broken exhaust line. There was also one three days period, when the software recording of  $\text{NH}_3$  signal was malfunctioning and data from that period was lost. The measured ship operates according to certain daily routine and pattern for  $\text{NH}_3$  concentration is very repeatable, though there are some variations in the level of the concentration. On 21.-23.12.2017 and 10.-12.1.2018 the daily basis urea consumption data recorded by the ship is low as well as the  $\text{NH}_3$  concentrations. From 13.1.2018 the urea consumption increases like the  $\text{NH}_3$  concentrations.

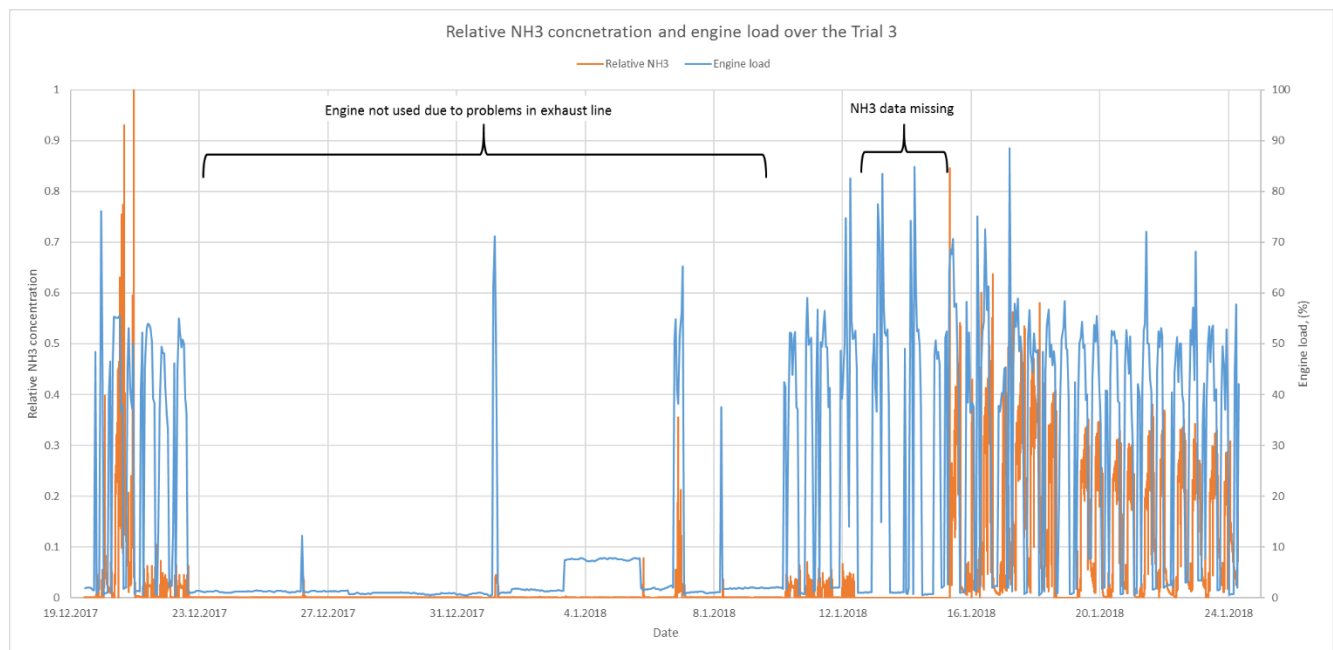


Figure 43. Relative  $\text{NH}_3$  concentration and engine load recorded during the Trial 3.

Trial 3 can be considered as successful. New installation probe worked in appropriate way and sensor was exposed to exhaust gas ca. 50 % of the ships operation time. Sensor measured very high  $\text{NH}_3$  concentrations and the comparison of its results with those obtained with FTIR were consistent with the experiences from trial 1. Sensor worked fine till the end of trial showing also concentrations below 5 ppm but at the laboratory it was found out that the all the sensor did not show any readings below ca. 4.5 ppm. Sensor needs further investigation for clarifying this problem with low concentrations.

### 5.3 Sulphur trioxide ( $\text{SO}_3$ ) screening

Sulphur in fuel is combusted almost completely to  $\text{SO}_2$ , which is seen as a correlation between measured  $\text{SO}_2$  concentrations in the engine-out exhaust and the sulphur content of fuel (Table 4). In maximum, a few percent of fuel sulphur is assumedly oxidised to  $\text{SO}_3$ . Elevated air to fuel ratios, or presence of vanadium and iron may enhance  $\text{SO}_3$  formation. At below 200 °C, all of the  $\text{SO}_3$  is present as sulphuric acid, while at above 500°C, it is almost entirely  $\text{SO}_3$ . Equilibrium towards sulphuric acid is favoured at higher water concentrations (Stuart 2010), (Neste 1987). At temperatures below the acid dew point, sulphuric acid aerosol is formed. The SCR systems may promote the  $\text{SO}_2$  oxidation to  $\text{SO}_3$ , which may result in higher sulphate levels in PM. Earlier studies have shown that conversion of  $\text{SO}_2$  to  $\text{SO}_3$  is less effective at lower temperatures (Lehtoranta, Vesala, et al. 2015) , (Aakko-Saksa, et al. 2017). Wet scrubbers tend to be ineffective in removing sulfuric acid aerosols due to the small size of the droplets (Stuart 2010). Reactions with other compounds may lead to other sulphates, for example ammonium sulphate or metal sulphates.

In our ISO 8178 PM filter sampling, dilution ratio used (10) favour condensation of sulphuric acid. The temperature of the diluted exhaust (42–52 °C) is lower than the dew point of sulphuric acid with

fuels used. High dilution ratios, for example 100, or hot sampling would be keep sample above the dew point of sulphuric acid (Figure 5.14 in (Aakko-Saksa, et al. 2017)). Sulphuric acid is not easily lost in sampling and handling of filter samples. There are methods to collect sulphates from exhaust completely for indirect determination of SO<sub>3</sub> as discussed in chapter 3.2. However, here we screened we screened the SO<sub>3</sub> concentration of exhaust based on the amount needed to accumulate measured SO<sub>4</sub> in PM (Table 4).

For E1 and E2 running on HFO, screened SO<sub>2</sub> conversion to SO<sub>3</sub> was well below 1%, although E2 was equipped with SCR that could induce SO<sub>3</sub> formation. For E2 using MGO fuel, respective conversion was almost 2%, and for E3 almost 4%. Concentrations of screened SO<sub>3</sub> were 2-5 mg/Sm<sup>3</sup> dry for E1 and E2 using HFO and 1 mg/Sm<sup>3</sup> dry for E2 using MGO. Respective SO<sub>3</sub> concentration was as high as 62 mg/Sm<sup>3</sup> dry for E3 using high-sulphur HFO. The sulphates present in PM before scrubber was used in these calculations. For an old marine engine in laboratory using fuels with various sulphur contents, conversion of SO<sub>2</sub> to SO<sub>3</sub> based on SO<sub>4</sub> in PM was 1-2.5% leading to the SO<sub>3</sub> concentrations up to 57 mg/Sm<sup>3</sup> dry exhaust gas.

Table 4. Calculated SO<sub>3</sub> concentrations in the exhaust based on measured SO<sub>4</sub> in PM.

Engine	Load	Fuel	Fuel S	SO <sub>2</sub>	SO <sub>4</sub> in PM <sup>b</sup>	SO <sub>3</sub>	SO <sub>3</sub> /
			%(m/m)	measured mg/Sm <sup>3</sup> dry	mg/Sm <sup>3</sup> dry	screened mg/Sm <sup>3</sup> dry	SO <sub>2</sub> %
<b>E1</b>	75%/40%	HFO	0.652	659/540	4,9/5,1 <sup>b</sup>	4,1/4,2	0,6/0,8
<b>E2</b>	75%/40%	HFO	0.652	605/548	3,8/2,8 <sup>b</sup>	3,2/2,3	0,5/0,4
<b>E2</b>	40%	MGO	0.078	53	1,2 <sup>b</sup>	1,0	1,9
<b>E3</b>	63-65%	HFO	1.86	1583	74,3 <sup>b</sup>	61,9	3,9
<b>Lab<sup>a</sup></b>	75%/25%		0.078	63/51	1,1/0,7	0,9/0,6	1,5/1,2
<b>Lab<sup>a</sup></b>	75%/25%		0.375	307/254	6,6/3,2	5,5/2,7	1,8/1,1
<b>Lab<sup>a</sup></b>	75%/25%		2.22	1912/1618	56,8/32,3	47,3/26,9	2,5/1,7

<sup>a</sup> Laboratory engine, Aakko-Saksa et al. (2017) <sup>b</sup> Before scrubber.

Figure 44 shows that screened SO<sub>3</sub> concentrations depend on the fuel sulphur content and engine load. Furthermore, SO<sub>3</sub> formation was higher for E3 than for the other engines. Exhaust gas temperature was higher for E3 (appr. 340 °C) than for E1 and E2 (appr. 300 °C). However, exhaust gas temperature was the highest for laboratory engine (appr. 360 °C at 75% load and 320 °C at 25% load). The consequently high SO<sub>3</sub> concentration for E3 cannot be explained by exhaust temperature only.



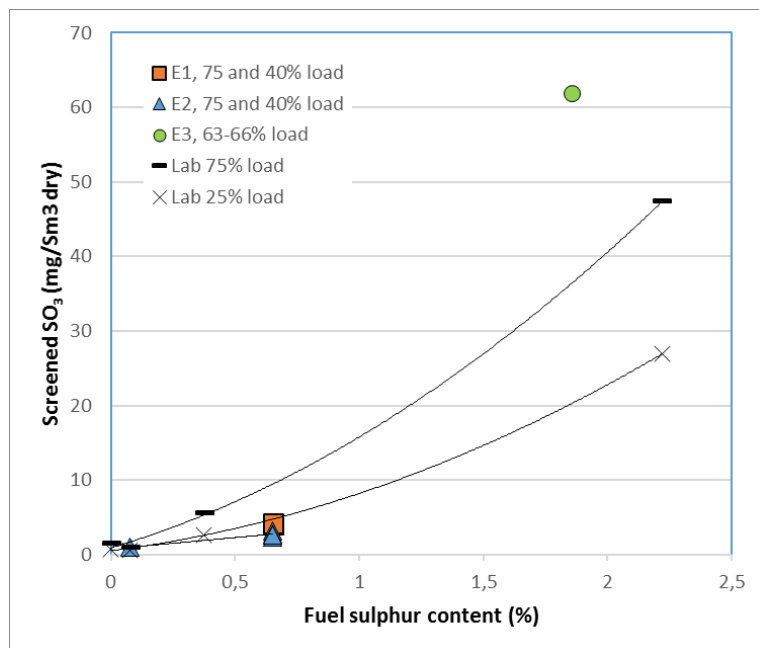


Figure 44. Relationship between screened SO<sub>3</sub> concentration, fuel sulphur content and engine load.

#### 5.4 Methane catalyst study

Prior to the ageing experiment, the catalyst was preconditioned at 400 °C and also the emissions were studied. The basic emission components upstream of the catalyst were already shown in Table 2. Downstream of the catalyst, the NO<sub>x</sub> was at the same level as upstream of the catalyst, as expected. As expected also, the temperature of 400 °C was too low to see any significant methane oxidation. However, the carbon monoxide (CO) was nearly totally oxidized with an efficiency of 98%.

During the ageing experiment the exhaust temperatures before and after the catalyst were followed. During the regeneration periods the added H<sub>2</sub> was found to react (oxidize) in the catalyst leading to remarkable temperature increase. The temperature downstream the catalyst was increased by 140 °C and 165 °C, at H<sub>2</sub> injection of 2% and 2.5%, respectively (Figure 45). The temperatures before the catalyst stayed constant regardless of hydrogen injection, as was targeted.

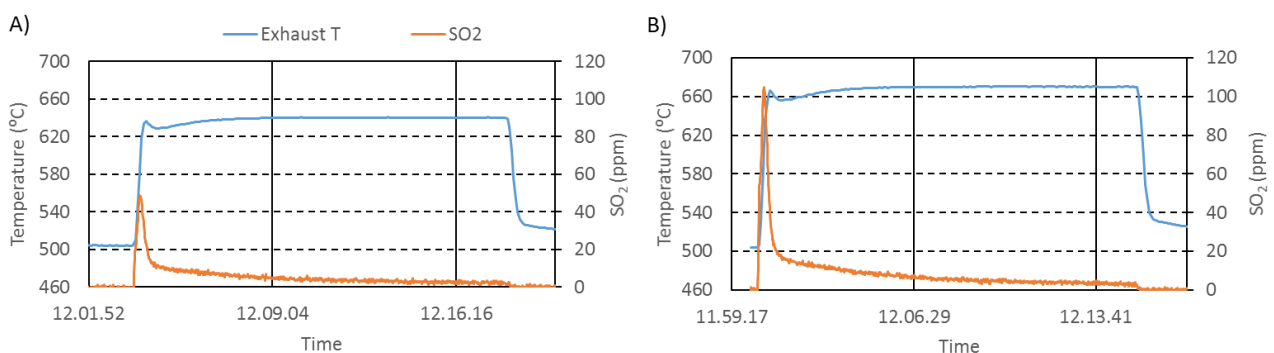


Figure 45. Exhaust temperature and SO<sub>2</sub> measured downstream of the catalyst during the regenerations A) with 2% H<sub>2</sub> and B) with 2.5% H<sub>2</sub>.

At each regeneration phase (i.e. H<sub>2</sub> addition) SO<sub>2</sub> was found to release from the catalyst since a sharp peak of SO<sub>2</sub> was measured downstream of the catalyst by FTIR. The SO<sub>2</sub> release seemed to depend also on the amount of added H<sub>2</sub> since at the higher H<sub>2</sub> amount also a higher SO<sub>2</sub> peak was observed (Figure 46).

An earlier study, done with the same engine facility, showed that the temperature increase alone (i.e. without any H<sub>2</sub> addition) did not release any SO<sub>2</sub> from the catalyst (Heikkilä 2017). Also earlier, a total reduced sulphur thermal converted to convert any H<sub>2</sub>S release to SO<sub>2</sub> was utilized, but since no hydrogen sulfide (H<sub>2</sub>S) was observed in the earlier study, the converted was not utilized in present study.

As targeted by the regeneration procedure, the H<sub>2</sub> addition and the following SO<sub>2</sub> release, was found to have an effect also on the methane efficiency of the catalyst. The methane conversion after the first 20 h ageing was found to be 37% (see Figure 46). After the following regeneration (2% H<sub>2</sub>) the conversion was found to be 44%. However, after the next 20 h ageing the conversion was decreased to level of 33%. Again, the methane conversion was recovered by the regeneration but resulted to lower level (i.e. 41%) than after the first regeneration (i.e. 44%). During the third ageing and regeneration process the same conversion decrease continued. However, after the fourth 20 h ageing the conversion seemed to maintain the same level that was observed after the third ageing. Following with a regeneration done by increased H<sub>2</sub> addition (2.5%) the conversion ended up to higher level than after the earlier regeneration.

The fifth ageing was a longer ageing of 70 h after which the methane conversion was found to decrease near to 21% while the following regeneration recovered the conversion to the level of 31%. The following two '20 h ageing and regeneration' -cycles resulted to nearly same methane conversion levels. This indicates that the catalyst is stabilized or saturated with the SO<sub>2</sub> meaning that no more SO<sub>2</sub> can be stored in the catalyst.

At the end (after 190 h), the temperature was increased from 500 °C to 550 °C and a significant increase was also found in the methane conversion which increased from 29% to 53%. One more ageing (20 h) was performed at this higher temperature resulting to methane conversion of 42% but the following regeneration recovered the conversion to nearly same level than before the ageing.

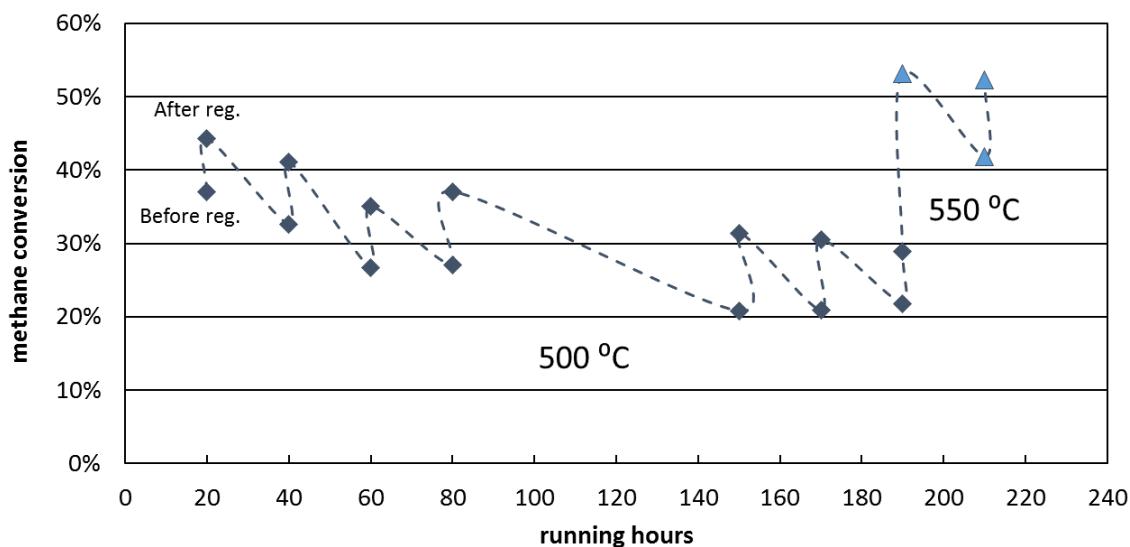


Figure 46. Methane conversion during the whole 190 h ageing at 500 °C, measured after the ageing period (before the regeneration) and after the regeneration (before next ageing), and additional 20 h ageing at 550 °C.

In addition to methane, some ethane and ethene were also found from the exhaust gas. The ethane concentration was near 10 ppm and ethene level was near 20 ppm. The ethene, being the easiest to oxidize, was, in practice, totally oxidized by the catalyst in all cases studied. The ethane behaved rather similarly to methane but the oxidation was found to be more effective. In the beginning of the experiment, the ethane conversion was above 90% and the lowest measured ethane conversion (at 150 h -190 h) was still above 60% (Figure 47).

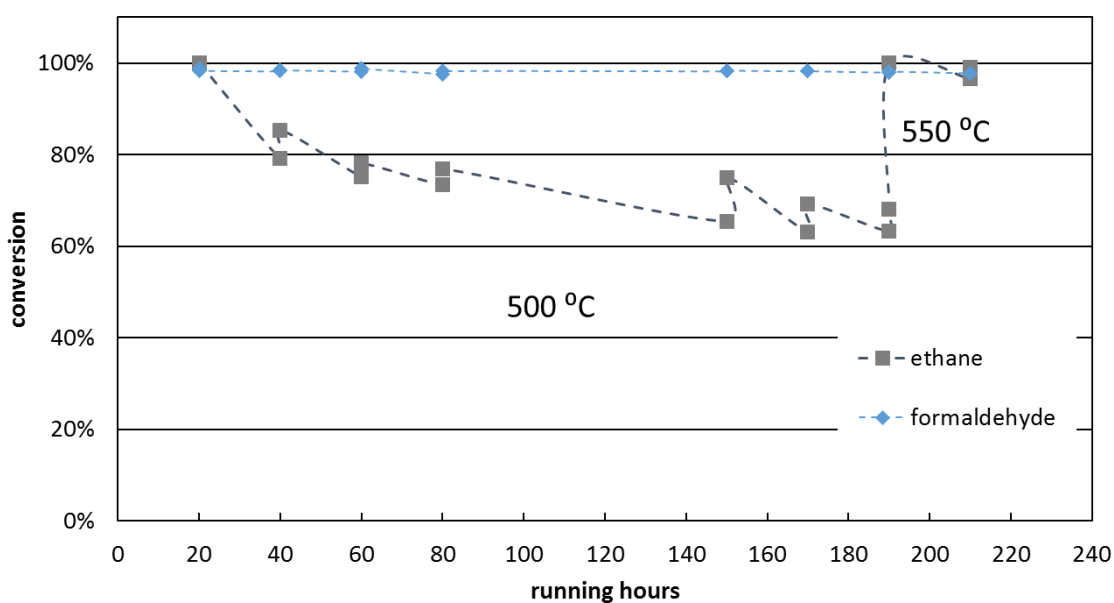


Figure 47. Ethane and formaldehyde conversions during the ageing experiment. Note. The lines are to guide eye only.

Regarding other emissions components than HC, the oxidation catalyst, as expected, did not affect the NO<sub>x</sub>. The CO was, in practice, totally oxidized by the catalyst in all cases studied. In addition, formaldehyde was measured from the exhaust with FTIR and was found to be approx. 50 ppm upstream of the catalyst. The formaldehyde was also nearly totally oxidized by the catalyst at all studied conditions as shown in figure Figure 48.

## 6 Conclusions

Hercules-2, Subproject 7.4: Emission measurement systems for integrated after-treatment technologies included several tasks, which were carried out by VTT. Tasks were:

- Desk-top work on emission regulation and SO<sub>3</sub> measurements methods
- Development of movable PM sampling system for ships
- Filter material study
- PM and PN measurements
- NH<sub>3</sub> sensor measurements
- Screening of SO<sub>3</sub> experimentally
- The methane catalyst study

SO<sub>3</sub> literature study covers recent development projects where the challenges of SO<sub>3</sub>/H<sub>2</sub>SO<sub>4</sub> measurements are considered, and also some commercial developments. These studies are related to extractive direct or indirect analysis of SO<sub>3</sub> in laboratory and in process conditions. Especially salt methods with NaCl and KCl which are based on extractive sampling and offline analysis were observed to give reliable results without any significant interference with SO<sub>2</sub>. In order to avoid challenges related to sample losses in sampling lines and one-point sampling one needs to make a through-duct in-situ measurement. In a study FTIR method was employed for this purpose in laboratory and in process conditions for direct measurement of SO<sub>3</sub>. The method was shown to operate in principle but more experimental verification is needed in process conditions.

From the on-board results, exhaust SO<sub>3</sub> concentrations were calculated based on the analysed sulphates from filters. Conditions in our extractive filter sampling favored condensation of sulphuric acid, and also other non-volatile sulphates are collected. For two marine engines running on HFO, the results indicated that below 1% of SO<sub>2</sub> converted to SO<sub>3</sub>, while almost 4% for one engine.

Moveable PM system for on-board measurement was needed due heavy and large size commercial systems meant for PM sampling. When performing PM measurements on-board the space is often very limited and if measurements are needed before and after aftertreatment devices, the PM device needs to be moved up and down between decks. At VTT a small movable PM-SDS was developed. System includes sampling unit, control unit and pump. The weights of the units are from 10 to 30 kg and sizes of the control and sampling units are ca. 60 x 40 x 25 cm. VTT's commercial PM sampling unit (AVL 472 Smart Sampler) consists of two units which weight 245 kg and 60 kg and corresponding dimensions are 73 x 64 x 164 cm and 75 x 56 x 153.

PM-SDS was verified at VTT's laboratory by performing comparison measurements with AVL Smart Sampler. With DRs 5 and 15 the result were equal (within  $\pm 2\%$ ) with AVL Smart Sampler. With DR of 10 the difference was almost 20% and the reason for that was not found, so a further work is still needed to for completing the verification of PM-SDS. It was also found that 15 is the highest recommended DR for PM-SDS.

Filter material study was performed with dual-fuel marine engine using LFO and marine engine on-board a ship using HFO as fuel. Measurements were carried out with four types of filter materials, two PTFE-types, one PTFE bonded glass fiber and one quartz quality filters. As a conclusion, PTFE bonded glass fiber filters, and particularly quartz filters, tend to collect more material than the PTFE filters. However, at low PM concentrations this difference was not always consistent.

PM and PN measurements were made on two on-board measurements campaigns from three engines using HFO and limited tests also with MGO. A dual-fuel marine engine was measured using natural gas and LFO. Results point out that fuel quality has significant influence on PM and PN emissions. Switching from HFO to low sulphur MGO or LFO decreased the PM emission roughly by 50% and further on using natural gas reduced PM emissions by over 85%. PM reduction over the scrubber was 17-45% The PN emissions were decreased by ca. 90% with MGO in comparison with HFO. With dual fuel engine, the PN emissions with natural gas were 99% lower compared to the diesel. The PN emissions (solid particles) before and after the scrubber were on the same level.

PN measurements also included comparison of legislative PN measurement method and Pegasor PPM-S particle sensor. Measurements were performed with dual-fuel engine in diesel and DF-modes using multiple engine loads. Results reveal that particle sensor needs application specific calibration for accurate results.

Comparison of different  $\text{NH}_3$  measurement techniques were performed at VTT's lab and in on-board measurements. The performance on  $\text{NH}_3$  sensors was the main interest. Sensor was compared against LDS and FTIR methods. The sensor is designed for automotive applications using high quality diesel fuel. The study with diesel bus showed that the results obtained with LDS and sensor are equal, while those obtained with FTIR were slightly lower. This is due to tendency of  $\text{NH}_3$  to adsorb to sampling lines and filters. With natural gas applications the sensor gives significantly, lower concentrations compared to LDS and FTIR though the sensor response is linear in comparison with other instruments. It needs to be highlighted that the sensor is not designed for natural gas applications.

Three on-board measurements campaigns were performed with the  $\text{NH}_3$  sensor. One of those included also FTIR measurements for comparison, and two others were long-term tests on ships. In all campaigns, HFO and low sulphur ( $\text{S} < 0.1\%$ ) fuels were used. The extractive FTIR method proved

to be very sensitive to SO<sub>2</sub> in exhaust when measuring NH<sub>3</sub>. In the presence of SO<sub>2</sub>, ammonium sulphate forms in the sampling system and the NH<sub>3</sub> concentrations are underestimated by FTIR. The long-term campaigns showed that NH<sub>3</sub> sensor has potential for monitoring of NH<sub>3</sub> in harsh conditions if precautions are used for protecting the sensor.

Catalyst study shows that with a methane oxidation catalyst a methane conversion of 50% can be reached with aged and regenerated catalyst at exhaust temperature of 550 °C.

The ageing experiments showed that during each 20 h ageing periods, the methane efficiency decreased. The regeneration, done by adding H<sub>2</sub> to the exhaust upstream of the catalyst releases SO<sub>2</sub> from the catalyst and recovers the methane oxidation capability to some extent. The SO<sub>2</sub> release was found to happen immediately after the H<sub>2</sub> injection was started indicating that even shorter H<sub>2</sub> injection times might result to same effect shown in this study done by 15 min H<sub>2</sub> injections.

The reactions of H<sub>2</sub> in the catalyst significantly increased the exhaust temperature downstream of the catalyst. This has to be taken into account if even higher exhaust temperatures would be relevant for methane catalyst utilization since too high temperature can destroy the catalyst operation.

This study showed that the H<sub>2</sub> assisted regeneration could be one way to recover the methane oxidation catalyst's performance. However, before taking this method to real applications, there are several issues to be studied further. At least the optimized H<sub>2</sub> amounts and regeneration intervals should be figured out as well as the H<sub>2</sub> availability and practical utilization in real application. Another issue is the catalyst efficiency for the methane oxidation, since the ones observed in present study might not be enough.

## **7 Acknowledgements**

The writers wish to thank the following VTT employees for their significant work in developing research facilities and during the laboratory and field experiments: Tommi Hangasmaa, Tuula Kajolinna, Mikko Kallio, Hannu Kuutti, Keijo Kähkönen, Jukka Lehtomäki, Reijo Mikkola, Ari-Pekka Pellikka and Pekka Piimäkorpi.

We also gratefully acknowledge the discussions with Sebastiaan Bleuanus and Jukka Leinonen from Wärtsilä Oyj during the planning and the course of the project, and Heikki Korpi and Juha Kortelainen from Wärtsilä Oyj Vaasa for their valuable help during the field experiments. We also thank Erkkä Saukko from Pegasor Oy for carrying out field experiments with PPS-M sensor and the data analysis.

## 8 References

- Aakko-Saksa, P, T Murtonen, H Vesala, P Koponen, H Timonen, K Teinilä, and M Aurela. 2017. "Black Carbon Emissions from a Ship Engine in Laboratory." SEA-EFFECTS BC WP1.
- ABB. 2018. *ABB Diodelaser for ammonia measurement*.  
[https://library.e.abb.com/public/8b93dfc8eb8a486eae239a2b9e21b601/AN\\_ANALYTICAL\\_LS4000\\_101\\_EN\\_B.pdf](https://library.e.abb.com/public/8b93dfc8eb8a486eae239a2b9e21b601/AN_ANALYTICAL_LS4000_101_EN_B.pdf).
- Alanen, J, E Saukko, K Lehtoranta, T Murtonen, H Timonen, R Hillamo, P Karjalainen, et al. 2015. "The formation and physical properties of the particle emissions from a natural gas engine." *Fuel* 155-161.
- Amanatidis, S, L Ntziachristos, B Giechaskiel, A Bergmann, and Z Samaras. 2014. "Impact of selective catalytic reduction on exhaust particle formation over excess ammonia events." *Environ. Sci. Technol.* 11527–11534.
- Amanatidis, Stavros. 2017. «Application of the dual Pegasor Particle Sensor to real-time.» *Journal of Aerosol Science* 93-104.
- Amanatidis, Stavros. 2016. «Measuring number, mass, and size of exhaust particles with diffusion chargers: The dual Pegasor Particle Sensor.» *Journal of Aerosol Science* 1-15.
- Anderson, M, K Salo, and E Fridell. 2015. "Particle- and Gaseous Emissions from an LNG Powered Ship." *Environmental Science & Technology* 49 (20) doi:10.1021/acs.est.5b02678 12568–75.
- Antson, Olli, Kati Lehtoranta, Hannu Vesala, and Harri Mustikkamäki. 2014. "Ammonia measurement challenges in SCR units." 11th International conference and exhibition on emission monitoring, May 14-16, 2014, Istanbul.
- Besch, Marc. 2016. *In-line, Real-time particulate Matter Sensors for OBD and Exhaust After-treatment System Control Applications*. Dissertation, West Virginia University.
- Bionda. 2002. «Flue Gas SO<sub>3</sub> Determination – Importance of Accurate Measurements in.» NETL Conference on SCR and SNCR Reduction NO<sub>x</sub> Control, Pittsburgh, PA, 2002.
- Breen. n.d. *AbS and SO<sub>3</sub> formation in Flue Gas Streams*. Πρόσβαση 2017. <http://breenes.com/solutions-services/acid-gas-products/absensor-so3/>.
- Cao. 2010. «Studies of the Fate of Sulfur Trioxide in Coal-Fired Utility Boilers.» *Environ. Sci. Tech.*
- CEMTEK Instruments. 2018. *CEMTEK Instruments*. <http://www.cemtekinstruments.com/instrumentswp/so2-so3-laser-analyzer/>.
- Chabot, Bob. 2010. «Opportunity NO<sub>x</sub>.» *Motor Magazine*.
- Chase, R, J Richert, D Lewis, M Matti Maric, Ning Xu, and G Duszkievicz. 2004. *PM Measurement Artifact: Organic Vapor Deposition on Different Filter Media*. SAE International 2004-01-0967,, SAE International.
- Chien, Yu-Chien. 2017. «Testing Methods for Continuous Monitoring of SO<sub>3</sub> and H<sub>2</sub>SO<sub>4</sub> at Flue gas conditions.» *26th ICDERS*. International Colloquium on the Dynamics of Explosion and Reactive Systems.
- Cordtz, Rasmus. 2013. «Cordtz R., Schramm J., Rabe R., Investigating SO<sub>3</sub> formation from the combustion of heavy fuel oil in a four-stroke medium-speed test engine.» *Energy & Fuels* 6279-6286.
- Dene C., Himes R. 2004. *Continuous Measurement Technologies for SO<sub>3</sub> and H<sub>2</sub>SO<sub>4</sub> in Coal-Fired Power Plants*. Technical report, EPRI.

- DieselNet. 2018. *International: IMO Marine Engine Regulations*.  
<https://www.dieselnet.com/standards/inter/imo.php>.
- DieselNet. Revision 2017.07. *PM Measurement: In-Situ Methods*. Ecopoint Inc. Revision 2017.07.
- EPA. 2018. *EPA Method 8: Determination of Sulfuric Acid and Sulfur Dioxide Emissions from Stationary Sources*. <https://www.epa.gov/homeland-security-research/epa-method-8-determination-sulfuric-acid-and-sulfur-dioxide-emissions>.
- EPRI. 2004. "Continuous Measurement Technologies for SO<sub>3</sub> and H<sub>2</sub>SO<sub>4</sub> in Coal-Fired Power Plants." Technical Report.
- EPRS . 2016. *Briefing: The IMO - for safe, secure and efficient shipping on clean oceans*.  
[http://www.europarl.europa.eu/RegData/etudes/BRIE/2016/577964/EPRS\\_BRI%282016%29577964\\_EN.pdf](http://www.europarl.europa.eu/RegData/etudes/BRIE/2016/577964/EPRS_BRI%282016%29577964_EN.pdf).
- EUR-Lex. 2016. *Regulation (EU) 2016/1628 of the European Parliament and of the Council* . Πρόσβαση 2018. <http://eur-lex.europa.eu/legal-content/en/TXT/?uri=CELEX:32016R1628>.
- Fateev, Clausen (ed), and Sonnik Clausen. 2016. *Sulfur trioxide measurement technique for SCR units*. Environment Project No. 1885, Ministry of Environment and Food of Denmark.
- FINAS. 2018. *ACCREDITED TESTING LABORATORY*. [www.finas.fi/Documents/T259\\_A11\\_2018.pdf](http://www.finas.fi/Documents/T259_A11_2018.pdf).
- Heikkilä, S. 2017. *Methane slip abatement by hydrogen addition*. Master's thesis, University of Vaasa.
- Hieta, Tuomas. 2014. «Simultaneous detection of SO<sub>2</sub>, SO<sub>3</sub> and H<sub>2</sub>O using QCL spectrometer for combustion applications.» *Applied Physics B* 847-854.
- IMO. 2017. *Nitrogen Oxides (NO<sub>x</sub>)- Regulation 13*.  
[http://www.imo.org/en/OurWork/environment/pollutionprevention/airpollution/pages/nitrogen-oxides-\(nox\)-%E2%80%93regulation-13.aspx](http://www.imo.org/en/OurWork/environment/pollutionprevention/airpollution/pages/nitrogen-oxides-(nox)-%E2%80%93regulation-13.aspx).
- . 2018. *NO<sub>x</sub> Technical Code 2008*.  
[http://www.imo.org/en/OurWork/Environment/PollutionPrevention/AirPollution/Documents/Air%20pollution/Resolution%20MEPC.177\(58\)%20NOx%20Technical%20Code%202008.pdf](http://www.imo.org/en/OurWork/Environment/PollutionPrevention/AirPollution/Documents/Air%20pollution/Resolution%20MEPC.177(58)%20NOx%20Technical%20Code%202008.pdf).
- . 2018. *Specific Emission Control Areas*.  
[http://www.imo.org/en/OurWork/Environment/PollutionPrevention/AirPollution/Pages/Emission-Control-Areas-\(ECAs\)-designated-under-regulation-13-of-MARPOL-Annex-VI-\(NOx-emission-control\).aspx](http://www.imo.org/en/OurWork/Environment/PollutionPrevention/AirPollution/Pages/Emission-Control-Areas-(ECAs)-designated-under-regulation-13-of-MARPOL-Annex-VI-(NOx-emission-control).aspx).
- IMO/Marpol. 2018. *MARPOL Annex VI revised*.  
[http://www.imo.org/en/KnowledgeCentre/IndexofIMOResolutions/Marine-Environment-Protection-Committee-\(MEPC\)/Documents/MEPC.176\(58\).pdf](http://www.imo.org/en/KnowledgeCentre/IndexofIMOResolutions/Marine-Environment-Protection-Committee-(MEPC)/Documents/MEPC.176(58).pdf).
- IMO/US. 2017. *Dieselnet*. <https://www.dieselnet.com/standards/us/marine.php>.
- IMO-Regulation 14. 2017.  
[http://www.imo.org/en/OurWork/Environment/PollutionPrevention/AirPollution/Pages/Sulphur-oxides-\(SOx\)-%E2%80%93Regulation-14.aspx](http://www.imo.org/en/OurWork/Environment/PollutionPrevention/AirPollution/Pages/Sulphur-oxides-(SOx)-%E2%80%93Regulation-14.aspx).
- Khalek, Imad. 2017. *Exhaust sensors: the solution for onboard diagnostics & emissions monitoring*. Motor Vehicle/Vessel Emission Control Workshop, Hong Kong 2016, Southwest Research Institute.
- Lehtoranta, K, T Murtonen, H Vesala, P Koponen, J Alanen, P Simonen, T Rönkkö , et al. 2017. "Natural gas engine emission reduction by catalysts." *Emiss. Control Sci. Technol.* 3 (2) 142-152.
- Lehtoranta, Kati. 2017. «Natural Gas Engine Emission Reduction by Catalysts.» *Emission Control Science and Technology*, 3(2) 142–152.





- UNECE. 2014. «Addendum, 15: Global technical regulation No. 15, Worldwide harmonized.»  
<https://www.unece.org/fileadmin/DAM/trans/main/wp29/wp29r-1998agr-rules/ECE-TRANS-180a15e.pdf>.
- . 2017. *Global Technical Regulations*.  
[https://www.unece.org/trans/main/wp29/wp29wgs/wp29gen/wp29glob\\_registry.html](https://www.unece.org/trans/main/wp29/wp29wgs/wp29gen/wp29glob_registry.html).
- . 2018. "UN Vehicle Regulation 83." <https://www.unece.org/trans/areas-of-work/vehicle-regulations/agreements-and-regulations/un-regulations-1958-agreement/regulations-addenda-to-the-1958-agreement/old-version-of-regulations-pages/regs-81-100.html>.
- Vainio, Emil. 2014. *Fate of Fuel-Bound Nitrogen and Sulfur in*. Åbo Akademi University.
- Wang. 2008. *Ammonia sensor for closed loop SCR control*. 2008-01-0919, SAE International.
- Wang, D. 2007. "Ammonia sensor for SCR NO<sub>x</sub> reduction." *2007 Diesel Engine-Efficiency & Emissions Research Conference (DEER 2007)*. U.S. Department of Energy's (DOE).
- Wemberg. 2011. «OXIDATION OF SO<sub>2</sub> to SO<sub>3</sub> over catalysts - optimizing conversion output.»
- Wemberg, Antti. 2014. «SO<sub>3</sub> katalyyttikokeet - jatkotestit.» MMEA report, VTT-R-01089-14.
- Wärtsilä. 2017. *Wärtsilä 20DF*. Πρόσβαση 2017. <https://www.wartsila.com/products/marine-oil-gas/engines-generating-sets/dual-fuel-engines/wartsila-20df>.
- Zetterdahl, Maria. 2016. «Particle Emissions from Ships.» *Thesis, Chalmers University of Technology, Gothenbur, Sweden 75*.
- Zheng. 2017. «Development and Experimental Evaluation of a Continuous Monitor for SO<sub>3</sub> measurement.» *Energy & Fuels* 9684-9692.
- Zheng, Z. 2011. «Investigation of solid particle number measurement :Existence and nature of sub-23 nm particles under PMP methodology.» *Journal of Aerosol Science* 42 (2011) 883–897 (Journal of Aerosol Science 42(2011)883–897) 883-897.